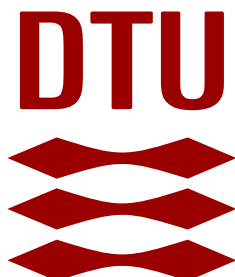


TECHNICAL AND ECONOMIC EVALUATION OF GEOTHERMAL DOUBLET SYSTEMS  
DESIGNS AND CONFIGURATIONS FOR HEAT PRODUCTION FROM LOW ENTHALPY  
SEDIMENTARY AQUIFERS



A Thesis by

LOPEZ TORRES LUIS FERNANDO

Supervised by

HAMID NICK, Danish Hydrocarbon Research and Technology Center

VERA ROCCA, Politecnico di Torino

Politecnico di Torino

Danish Hydrocarbon Research and Technology Center

Denmark Technical University

MASTER OF SCIENCE

OCTOBER 2019

Major Subject: Geothermal energy.

## Abstract

The last couple of decade's geothermal energy production from hot sedimentary aquifers (HSA) has become one of the most common alternative solution for the direct heating. The most used technique to exploit HSA has been hydrothermal system, better known as doublets systems, in which there is at least one production and one injection well. Therefore, the correct choice of well type among the available options and accurate setting of doublet system configuration turn into a sensitive aspect in the increment of energy recovery. The current study aims to evaluate and compare different well types: vertical, horizontal and multilateral (Using the technique Radial Jet Drilling – RJD) wells to find an efficient exploitation scenario. To this end, different doublet configuration in both homogenous and heterogeneous aquifers are considered. Several key performance indicators such as doublet lifetime, required pump pressure, net energy and NPV are considered to compare technically and economically viability of the different cases.

Results indicate that replacing the traditional vertical wells for horizontal one in doublet systems is capable of generating important reductions in energy losses. That depending on the length of the horizontal section can reach up to 80% of improvement. Producing a boost in NPV of minimum 10% until being from seven to eight times higher than traditional doublets, either in the short (Drop of 1°C) or long term (Drop of 10°C). The outcomes from this study underline the advantages of horizontal well system for exploiting HSA economically. Which have not been studied yet.

*Keywords:* Geothermal doublets - horizontal/multilateral wells - numerical modelling – NPV

## TABLE OF CONTENTS

Abstract.....	2
1. METHODOLOGY .....	8
1.1 Flow and Heat Transfer Modelling.....	8
1.2 Model Validation.....	10
1.3 Net Present Value Model .....	12
1.4 Parameter Analysis.....	13
1.5 Heterogeneous Model .....	14
2. RESULTS.....	16
2.1 Homogeneous Model .....	16
2.1.1 Vertical well system (V-S) .....	16
2.1.2 Horizontal well system (Hz-S).....	18
2.1.3 Comparison V-S to Hz-S.....	20
2.1.4 Comparison Hz-S to MLT-S .....	25
2.2 Heterogeneous Model .....	28
2.2.1 Heterogeneity – $k_1$ .....	28
2.2.2 Heterogeneity – $k_2$ .....	29
2.2.3 Heterogeneity – $k_3$ .....	31
3. CONCLUSIONS.....	34
References.....	36

## TABLE OF FIGURES

<b>Figure 1</b> Example of layout of the general doublets systems set. ....	8
<b>Figure 2</b> Analytical solution versus Comsol 2D solution .....	11
<b>Figure 3 - a.</b> Temperature breakthrough for 2D and 3D realizations – <b>b.</b> Schema 3D model .....	11
<b>Figure 4</b> Heterogeneity models .....	15
<b>Figure 5 a.</b> Production temperature profile at different pumping rates and doublet configuration. <b>b.</b> Average temperature at boundaries.....	17
<b>Figure 6</b> Development of aquifer temperature for two adjacent single doublets for tramline and checkboard configurations.....	17
<b>Figure 7</b> Schematic layout of Horizontal doublet system configuration. Red stands for producer well and blue for injector well. ....	18
<b>Figure 8 .</b> Production temperature profile at different pumping rates). ....	19
<b>Figure 9</b> Differential pumping pressure for Hz-S. ....	19
<b>Figure 10</b> Comparison of $T_p$ for Hz-S and V-S.....	20
<b>Figure 11</b> Temperature plume development for V-S and Hz-S ( $Q_{V-S3}/Q_{Hz-S3}$ ).....	21
<b>Figure 12</b> Differential pumping pressure comparison between V-S and Hz-S.....	22
<b>Figure 13</b> Key parameters comparison between V-S and Hz-S.....	24
<b>Figure 14</b> Key parameters comparison between V-S and Hz-S, second part.....	25
<b>Figure 15</b> Temperature and differential pumping pressure profiles at 200m <sup>3</sup> /h.....	26
<b>Figure 16</b> Temperature plume development (°C) for V-S and MLT-S with a pumping rate of 100m <sup>3</sup> /h per well.....	27
<b>Figure 17</b> Key parameters comparison between Hz-S (V-S) and MLT-S-S at 200m <sup>3</sup> /h.....	27
<b>Figure 18</b> Temperature and differential pumping pressure for different systems in $k_1$ .....	29

<b>Figure 19</b> Temperature development during 30 years for V-S, Hz-S (L_Hz <sub>2</sub> – Location 1) and MLT-S for a total pumping rate of 600m <sup>3</sup> /h in k <sub>1</sub> . .....	29
<b>Figure 20</b> Temperature and Pressure profile for different systems in k <sub>2</sub> .....	30
<b>Figure 21</b> Temperature development during 30 years for V-S, Hz-S (L_Hz <sub>2</sub> – L_Hz <sub>3</sub> ) and MLT-S for a total pumping rate of 600m <sup>3</sup> /h in k <sub>2</sub> . .....	32
<b>Figure 22</b> Temperature and differential pumping pressure for different systems in k <sub>3</sub> .....	33
<b>Figure 23</b> Temperature development during 30 years for V-S, Hz-S (L_Hz <sub>2</sub> – Location 1) and MLT-S for a total pumping rate of 600m <sup>3</sup> /h in k <sub>2</sub> . .....	33

## Introduction

Production of geothermal energy in the Netherlands has received a lot of attention, since the first doublets projects was complete in 2007 [1] in the West Netherland Basin (WNB) with the producing targets depth are in between 2000m and 2500m and an initial temperature ranging from 70 to 90 °C [2]. There have been several studies to evaluate diverse parameters. Such as water viscosity and density temperature dependent [3] [4], aquifer porosity and permeability [5] [6], production/injection flow rates [7], injection temperature [8], reservoir geometry [9] and doublets system pattern (Tramline/Checkboard) that affect heat exchange and doublet lifetime in geothermal reservoirs [10]. Even though, previous studies addressed the effect of doublets patterns in system lifetime (LT), differential pumping pressure ( $\Delta P$ ), net energy ( $E_{net}$ ) and net present value (NPV). The performance of doublet system utilizing different well types and doublet configuration used in conjunction with variations of flow rates, doublet patterns and rock anisotropy has not been studied.

The main objective of the current study rely on the technical and economic comparison of producing geothermal energy through vertical or horizontal wells and insights about using multilateral wells as exploitation system. Taking into account changes of flow rates, wells diameter, well location and rock properties (Porosity and Permeability). Three cases are considered in this study to perform this evaluation. The cases are, **1) Vertical well system (V-S)**: Two vertical doublet for both tramline (Producers and injectors wells aligned) and checkboard (wells are alternated based on the “5-spot well layout” in the hydrocarbon industry [11]) configurations. **2) Horizontal well system (Hz-S)**: Horizontal doublet varying the wells location related to the top and bottom boundary of the aquifer and changing horizontal length for production/injection (100m, 500m and 1000m). **3) Multilateral well system (MLT-S)**: Two vertical doublet plus four laterals (100m/lateral) in each well with checkboard pattern, since lifetime and injectivity are enhanced by producing in this configuration [12].

Several key performance indicators such as doublet lifetime, required pump energy, net energy and NPV are considered to compare technically and economically viability of the different cases. Considering modifications on well type and doublet configuration; such as well diameter and horizontal length in case of Hz-S to produce at least the same amount of energy than V-S. As well as, the evaluation of MLT-S performances, compare to the other two systems. In the same way, coupling multi-parameter sensitivity and rock properties variations will give a more

comprehensive knowledge about general (Well/doublet configurations and rock properties) and specific (well diameters/locations and rates) information to plan a priori more cost-effective doublets systems.

## 1. METHODOLOGY

Several simulations using a 3D finite element (FE) approach performed to test different scenarios for HSA exploitation, which are (**Figure 1**):

- Vertical system (V-S): Two vertical doublet both tramline and checkboard pattern.
- Horizontal system (Hz-S): Horizontal doublet varying the well location and horizontal length.
- Multilateral system (MLT-S): Two vertical doublet plus four laterals set at the middle of the well.

These scenarios were applied for both homogenous and heterogeneous aquifers, by varying different human controlled parameters such as production rates, well location/diameters and system pattern. Well spacing ( $L$ ) that stands for the distance between producer/injector well and doublet spacing ( $dx$ ), which is the distance between two adjacent doublets [12] have kept constant in all simulations. According to the result obtained from these simulations, it was evaluated the performance of each sensitivity in terms doublet lifetime, differential pumping pressure, net energy, sweep and NPV. As well as, comparisons among the systems in order to identify main advantages and/or disadvantages from each of them.

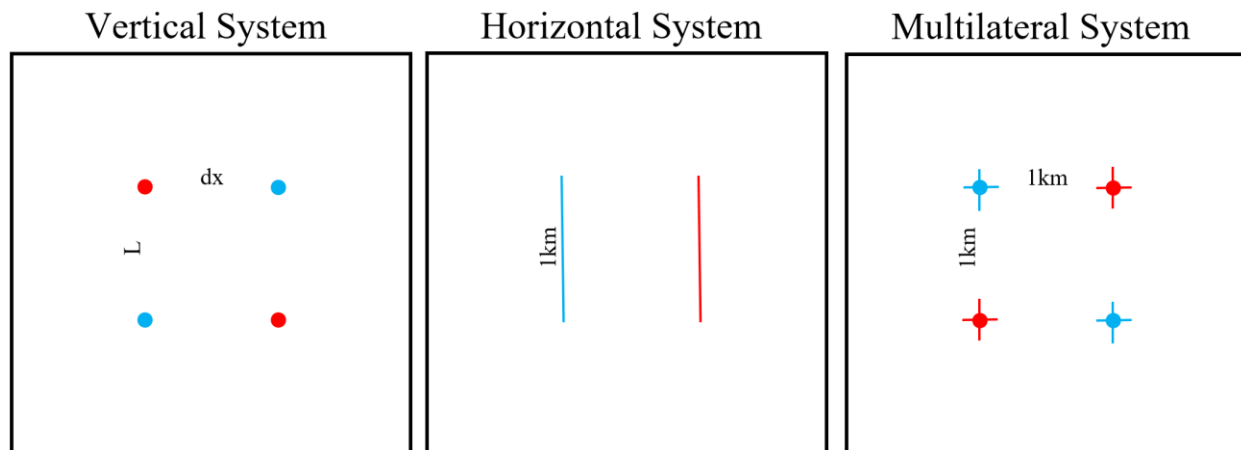


**Figure 1** Example of layout of the general doublets systems set. Checkboard pattern for Vertical and Multilateral systems. Red stands for producer well and blue for injector well. Top View.

### 1.1 Flow and Heat Transfer Modelling

An aquifer zone of 3km x 3km and 100m thickness sealed by under and over burden rocks. It is the so-called homogenous model for the purpose of this study. Aquifer properties have been

correlated to the Nieuwerkerk Formation data [13] [14] [15], listed in the **Table 1**. Isotropic properties and rock matrix flow with no presence of fracture have assumed.

Parameter	Description	Value	Units
$k_a$	Aquifer Permeability	1000	mD
$\phi_a$	Aquifer Porosity	0.1	-
$\lambda_a$	Aquifer Conductivity	2.7	W/m/K
$C_a$	Aquifer specific heat capacity	730	J/kg/K
$\rho_a$	Aquifer density	2650	kg/m <sup>3</sup>
$k_s$	Under/over burden shale Permeability	0.001	mD
$\phi_s$	Under/over burden shale Porosity	0.05	-
$\lambda_s$	Under/over burden shale Conductivity	2.0	W/m/K
$C_s$	Under/over burden shale specific heat capacity	950	J/kg/K
$\rho_s$	Under/over burden shale density	2600	kg/m <sup>3</sup>
$C_w$	Water specific heat capacity	4200	J/kg/K
$\rho_w$	Water shale density	1050	kg/m <sup>3</sup>
GG	Geothermal gradient	30	°C/km
$T_{inj}$	Injection temperature	40	°C

**Table 1** List of parameters – Homogenous model

Dynamic flow and heat transfer modelling performed as the approach of Refs. [5] [16] [12]. A rigid medium completely water saturated where there is thermal equilibrium between fluid and solid phases, meaning  $\rho C \partial / \partial t T + \rho_w C_w \nabla (q T) - \nabla (\lambda \nabla T) = 0$ . Where, t [s] is time, T [K] is temperature,  $\rho$  [kg/m<sup>3</sup>] is mass density,  $C_w$  [J/(kg K)] is water specific heat capacity,  $\lambda$  [W/(m K)] is the thermal conductivity tensor, and  $\mathbf{q}$  [m/s] stands for the Darcy velocity vector. As well as, thermal conductivity given by  $\lambda_{eq} \mathbf{I} + \lambda_{dis}$ , where  $\lambda_{dis}$  is the thermal dispersion coefficient and  $\mathbf{I}$  the identity matrix; and volumetric heat capacity is in terms of the local average volume. It assumed  $\lambda_{eq}$  in the form of  $(1-\phi) \lambda_s + \phi \lambda_w$  and  $\rho C$  as  $(1-\phi) \rho_s C_s + \phi \rho_w C_w$  ( $\phi$  is porosity) which describe the equivalent heat conductivity, density and volumetric heat capacity as temperature independent. The thermal conductivity tensor given by  $\lambda = \lambda_{eq} + (\alpha_L) |\mathbf{q}| \mathbf{I} + \rho_f C_f (\alpha_L - \alpha_T) \mathbf{q} \mathbf{q} / |\mathbf{q}|$ . Where  $\alpha_L$  and  $\alpha_T$  stands for longitudinal and transversal direction of thermal dispersion coefficients, respectively. Darcy flow velocity resolved by  $\mathbf{q} = (k \nabla P) / \mu$ , where k [m<sup>2</sup>] is the intrinsic permeability,  $\mu$  [Pa s] the viscosity and P [Pa] the pressure. Viscosity temperature dependent has taken into account, since it has been demonstrated an important effect on the cold-water plume advance, therefore the method applied by refs [4] [16] [12] is accounted.

Spatial discretization was based on tetrahedral elements near to the well(s) and quadrilateral elements far from the doublet system, which range varies between 0.1m to 80m. The performed simulations give production temperature along time and pressure requirements according to injection/production flow rates and system parameters. Using the difference between injection and production pressure ( $\Delta P$ ) is estimated the pump energy losses ( $E_{\text{pump}}$ ), which is given by  $\int_0^{LT} \frac{Q \Delta P}{\varepsilon} dt$  (e.g [17]), where  $Q$  is production rate,  $LT$  is the lifetime and  $\varepsilon$  as the pump efficiency (60%). In same way, with the difference between injection (30°C) and production temperature ( $\Delta T$ ) is calculated the produced energy ( $E_{\text{prod}}$ ) by  $\int_0^{LT} Q \rho_w C_w \Delta T dt$  (e.g [17]). By means of this energy difference is obtained the net energy ( $E_{\text{net}}$ ) produced by the system.

## 1.2 Model Validation

The analytical solution developed by Barends et al [18] has been applied. This solution was compared with the one provided by Comsol Multiphysics, when a homogenous system is setting as 2D model. Parameters used are listed in the **Table 1**.

In this 2D model, it set a traditional doublet system into a rectangular model of 100m x 3km. Which represent an aquifer zone of 100m thick. Injector and producer wells are located in the middle of the system separated 1000m from each other. Cold water was injected at 30 °C and production temperature has monitored over time. Short edges at aquifer level set as a constant pressure boundaries and the long boundaries (top and bottom) were considered as no flow and insulated boundaries (see **Figure 3**). Besides fluid and rock properties were assumed not temperature dependent in order to simplify calculations.

It seen in **Figure 2** that exit a good fit among the solutions provided. Percentage of difference calculated between analytical and Comsol 2D does not exceed 7% along 100 years that was the time-step set.

With the purpose to minimize the uncertainties related to the simplifications done by the 2D solutions and constant properties assumptions. A 3D model of 3km x 1km composed by 3 layers was built. Where an aquifer of 100m thick is in between an over and under-burden sealing rocks of 200m each one. Cold water injected (30°C) at pumping rate of 100 m<sup>3</sup>/h and temperature dependency of fluid density and viscosity were taken into account. **Figure 3** shows that there is a small difference between the realizations with and without density driven flow [10] [12] [19].

Whereas, with variable viscosity caused by temperature dependency makes a noticeable difference among the 2D-constant properties and 3D realizations. Moreover, the presence of a top and bottom sealing rock impact over heat exchange process in the medium, reason by which the drop of production temperature after thermal breakthrough is softer than 2D solutions.

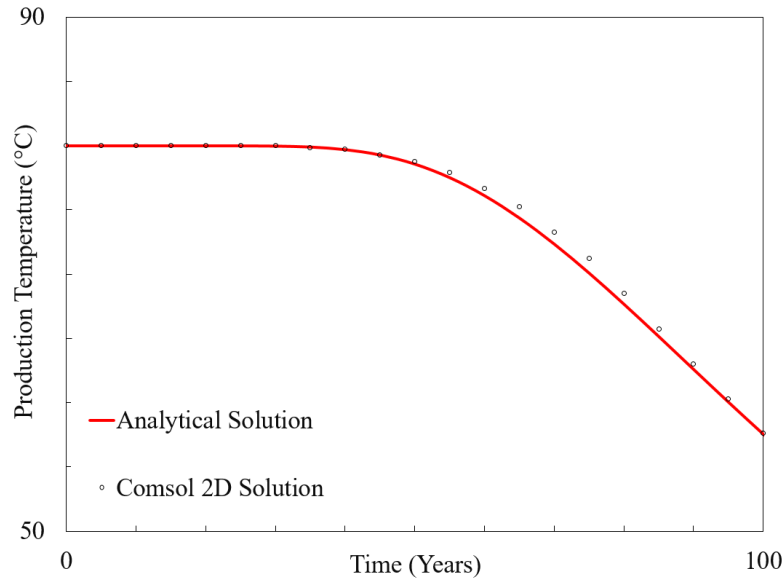


**Figure 2** Analytical solution versus Comsol 2D solution

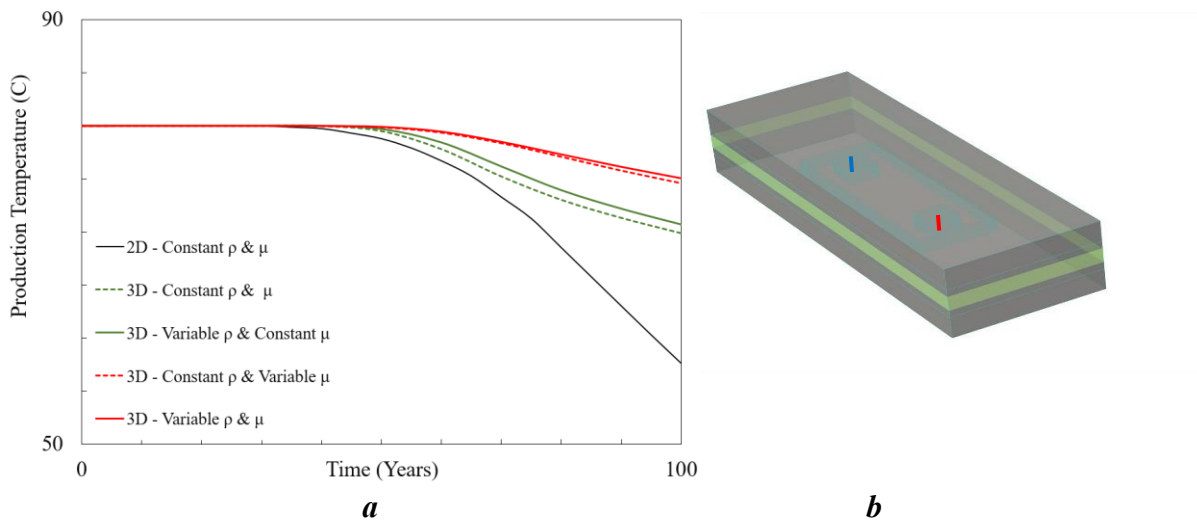


**Figure 3 - a.** Temperature breakthrough for 2D and 3D realizations – **b.** Schema 3D model

Taking into account results showed by **Figure 3a**. All realizations were set as the 3D model described and water properties (Density and Viscosity) dependent on temperature variation.

### 1.3 Net Present Value Model

The NPV model generated by Wees et al [20] has been used in this study for the purpose of economic evaluation and comparison among the different scenarios. The input data for this model are the net energy calculated from the simulations done and the economic parameters mentioned in the **Table 2**. Model is based on the Dutch scheme for geothermal energy exploitation. Therefore, it includes a feed-in tariff (SDE +) [14]. Extra costs due to separator installation has taken into account, since WNB doublets have shown natural gas co-production [12]. As well as, pump work-over cost and down time of about 40% due to maintenance have been accounted.

Aforementioned model works perfectly when the wells involved are vertical. Reason by which it has accounted an additional cost related to the horizontal length to be drilled [21] and multilateral drilling that for this study is related to Radial Jet Drilling (RJD). NPV was accumulated at 15years of production, since is the period of which SDE+ applies [22].

<b>Parameter</b>	<b>Value</b>	<b>Unit</b>
Heat Price [23]	7	€/GJ
Electricity price for operations [23]	20.55	€/GJ
Discount rate	7	%
<b>CAPEX</b>		
Well costs vertical section	1.5	M€/km
Well costs horizontal section	2.8	M€/km
Additional cost due to RJD	0.3	M€
Pump	0.5	M€
Separator	0.1	M€
Heat exchanger	0.1	M€
Contingency costs	0.89	M€
SEI (Drilling insurance)	0.69	M€
OPEX	5	% of Capex/year
Tax	26	%
<b>Feed-in Tariff (SDE+)</b>		
Base Energy Price [22]	0.052	€/kWh
Contribution SDE+	14.4	€/GJ

**Table 2** NPV – Economic parameters.

It is worth to mention that for the horizontal system scenarios. An increment in CAPEX account is taken into consideration due to the upscaling of well diameter and surface facilities, since it is expected that a single horizontal doublet handles the same amount of fluid that a two single vertical adjacent doublets. Meaning, that an increment of 5, 12 and 35% is accounted for 100, 500 and 1000m of horizontal length, respectively [23].

### 1.4 Parameter Analysis

Different sensitivities have been done where the main sensitivities it can be found in the injection/production flow rates among 200 to 600 m<sup>3</sup>/h depending on the doublet configuration. Well diameter varied from 10 to 20cm for the vertical & horizontal system. Being the smallest diameter coupled to the smallest pumping rate and so on. In multilateral system was implemented a unique well diameter (10cm) for simplicity. Well relative location respect to the top and bottom boundaries of the aquifer was varied, for the case of the horizontal system. **Table 3** lists more detailed the aforementioned parameters

Parameter	Description	Value	Unit
L	Well spacing	1000	m
dx	Doublet spacing	1000	m
<i>Vertical System (V_S)</i>			
Q	Flow rate/well	Q <sub>v-s1</sub> = 100 Q <sub>v-s2</sub> = 200 Q <sub>v-s3</sub> = 300	m <sup>3</sup> /h
d <sub>w</sub>	Well diameter	d <sub>w1</sub> = 10 d <sub>w2</sub> = 15 d <sub>w3</sub> = 20	cm
<i>Horizontal System (Hz_S)</i>			
Q	Flow rate/well	Q <sub>Hz-s1</sub> = 200 Q <sub>Hz-s2</sub> = 400 Q <sub>Hz-s3</sub> = 600	m <sup>3</sup> /h
d <sub>w</sub>	Well diameter	d <sub>w1</sub> = 10 d <sub>w2</sub> = 15 d <sub>w3</sub> = 20	cm
Location 1	Producer/Injector depth	Mid-depth aquifer 2500m	-
Location 2	Producer depth	10m to the top boundary	
	Injector depth	10m to the bottom boundary	
L_Hz	Horizontal Longitude	L_Hz1 = 100 L_Hz2 = 500 L_Hz3 = 1000	m

Parameter	Description	Value	Unit
<i>Multilateral System (MLT_S)</i>			
Q	Flow rate/well	$Q_{MLT-S} = 100$	m <sup>3</sup> /h
d <sub>w</sub>	Well diameter	d <sub>w1</sub> = 10	cm
La	Lateral length	100	m

*Table 3 Multy-parameter variations*

### 1.5 Heterogeneous Model

Based on the same 3D model geometry built for the homogenous realizations. It populated porosity and permeability heterogeneity according to what would be expected to find in sedimentary fluvial reservoirs encountered in the West Netherlands Basin [13]. Targeting to visualize and get insights how it affects the setting up of the different doublets configurations.

Applying the model developed by Olaf A. Cirpka. Which is capable of generating random auto correlated fields. “Method is based on the discrete Fourier transformation”, where the realizations are result of the back-transformation of power and phase spectrum to a physical domain, reason by which the fields obtained are periodic [24].

Aforementioned approach was applied to generate a random field for porosity distribution. It was generated three different heterogeneity distributions, which have an average porosity of 16%. An initial model with a variance of 0.04 was set as k<sub>1</sub>, having an average permeability of 1700mD. For a second model (k<sub>2</sub>) it was used a variance of 0.1 (Highly heterogeneous system) getting an average permeability of 1400mD and a third model was created with alto 0.1 of variance, however the direction of channels were inclined 45° degrees respect to the well spacing direction (k<sub>3</sub>) (See **Figure 4a – b - c**, respectively). Spatial correlation was kept constant with 700m in x-direction, 50m in y-direction and 1m in z-direction. Subsequently, permeability distribution was derived using the following **Equation 1** developed by Masoud et al [25].

$$k = -2.03 \times 10^{-7} \phi^5 + 2.55 \times 10^{-5} \phi^4 - 1.04 \times 10^{-3} \phi^3 + 8.91 \times 10^{-3} \phi^2 + 3.58 \times 10^{-1} \phi - 3.21$$

*Equation 1 Calculation of Permeability distribution*

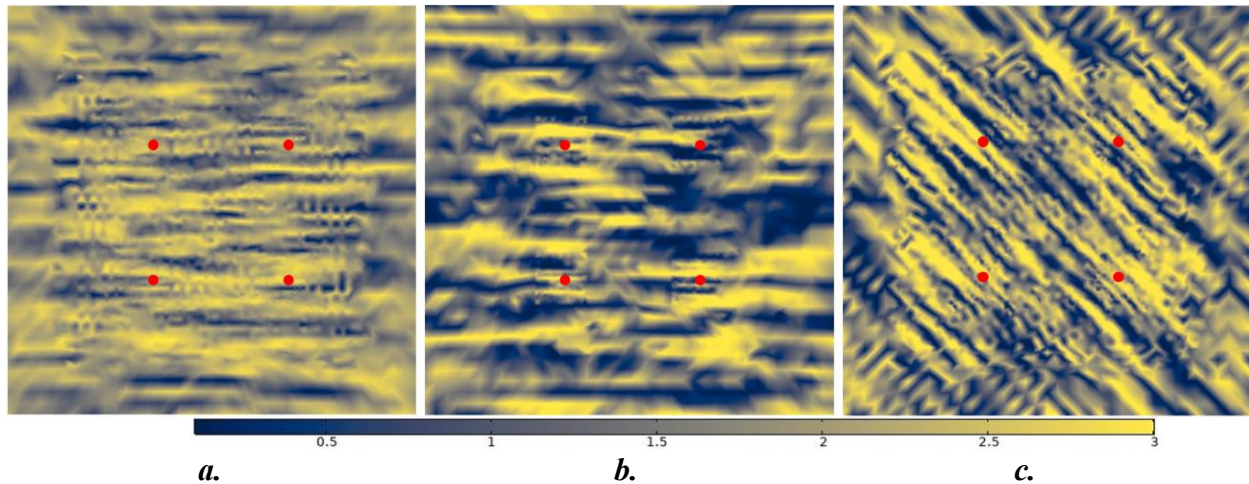


**Figure 4** Heterogeneity models

**a – b - c.** Permeability [D] slices at 2500m (Mid-point of the aquifer) for  $k_1$ ,  $k_2$  and  $k_3$ . Respectively. Red dots stand for the location of the wells.

**Figure 4** shows a slices at 2500m depth, which correspond to the average mid depth of the aquifer, of the random field of permeability generated. Where, dark grey represents the lowest limit and bright yellow for the highest, 0.001 to 3000mD, respectively.

## 2. RESULTS

The following chapter shows the outcomes obtained from several realizations. Starting for the comparison of the different well types and configurations in the homogenous model. Afterwards, it can be find the analysis respect to the heterogeneous one.

### 2.1 Homogeneous Model

#### 2.1.1 Vertical well system (V-S)

Realizations in tramline and checkboard were conducted at different pumping rates ( $Q_{v-s}$ ) and well diameters ( $d_w$ ). **Figure 5a** shows the average production temperature ( $T_p$ ) between two adjacent doublets for the mentioned parameters. Taking into account that the lifetime of the doublet system due to production temperature is when  $T_p$  decreases in  $5^\circ\text{C}$  ( $LT^5$ ), from the initial aquifer temperature ( $80^\circ\text{C}$  in average for this study). For both configuration, it observed that at low pumping rates,  $LT^5$  is much longer than high rates. For instance, at  $Q_{v-s1}$ , lifetime of the system is 110 years. While, increasing the pumping rates in 100% ( $Q_{v-s2}$ ) and 200% ( $Q_{v-s3}$ ), lifetime is being reduced around 60 and 80 years, respectively. In addition, it sees that the thermal breakthrough in checkboard configuration is delayed between two to four years compared to tramline configuration, no matter at which pumping rate is producing the system. However, as it was point it out by Willems et al in their study of interferences in heat exploitation [12]. After the thermal breakthrough, drop of  $T_p$  is faster (between  $2$  and  $3^\circ\text{C}$  per decade) than tramline configuration, which is more noticeable at high rates.

On the other hand, lifetime of a doublet system can be given also by the average temperature at the boundaries of the license area ( $LT_B = \text{Temperature decreases } 1^\circ\text{C}$ ). This area is estimated as two times the well spacing ( $L$ ) by two times doublets spacing ( $dx$ ). **Figure 5b** shows that not only  $LT_B$  like  $LT_p$  is longer for low pumping rates, being 50% greater for  $Q_{v-s1}$  than  $Q_{v-s2}$ . But also,  $LT_B$  in checkboard is prolonged several years due to the injector wells are located in opposite sides with respect to a specific boundary. Which makes that the average temperature drop at the boundaries will be delayed compare to tramline configuration.

Important to mention that interferences between doublets exist in both configurations. For the case of tramline configuration (**Figure 6 - Tramline**), as the cold-water front advances, the plume starts to show a teardrop shape that is becoming asymmetrical as getting close to the producer well it is, due to the presence of the second doublet system. This behavior is more

appreciable in checkboard configuration, even at early production stages (**Figure 6A'**). It sees that the plumes are deformed in direction (2-directions) towards to a single producer well. This explain why after the thermal breakthrough, the temperature drop is faster than tramline pattern.

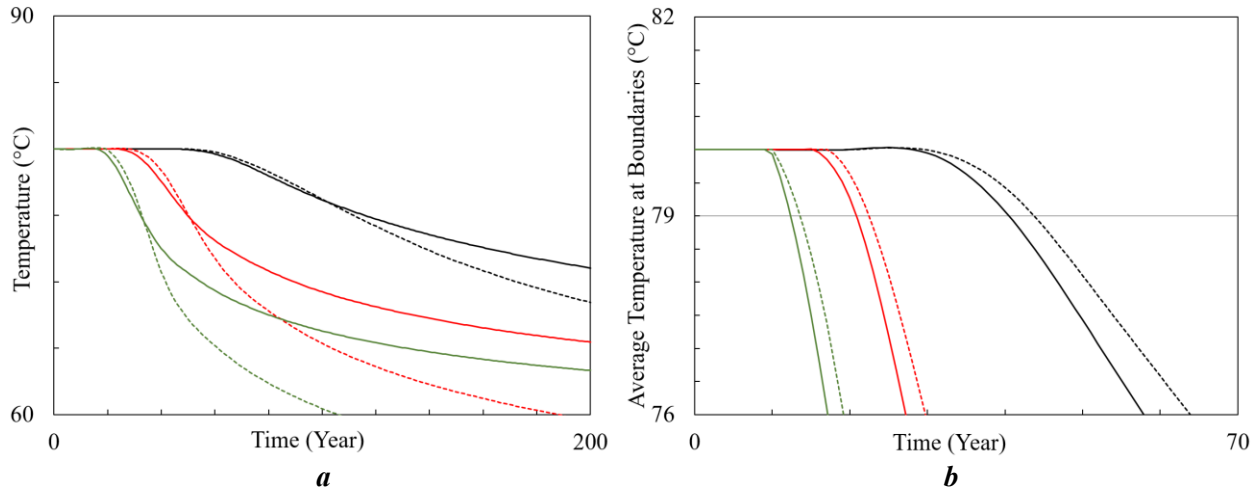


**Figure 5 a.** Production temperature profile at different pumping rates and doublet configuration. **b.** Average temperature at boundaries.

For both figures, continue lines represent tramline configuration and dashed lines are for checkboard configuration. Black color stands for  $Q_{v-s1}$ , red color for  $Q_{v-s2}$  and green color for  $Q_{v-s3}$ .

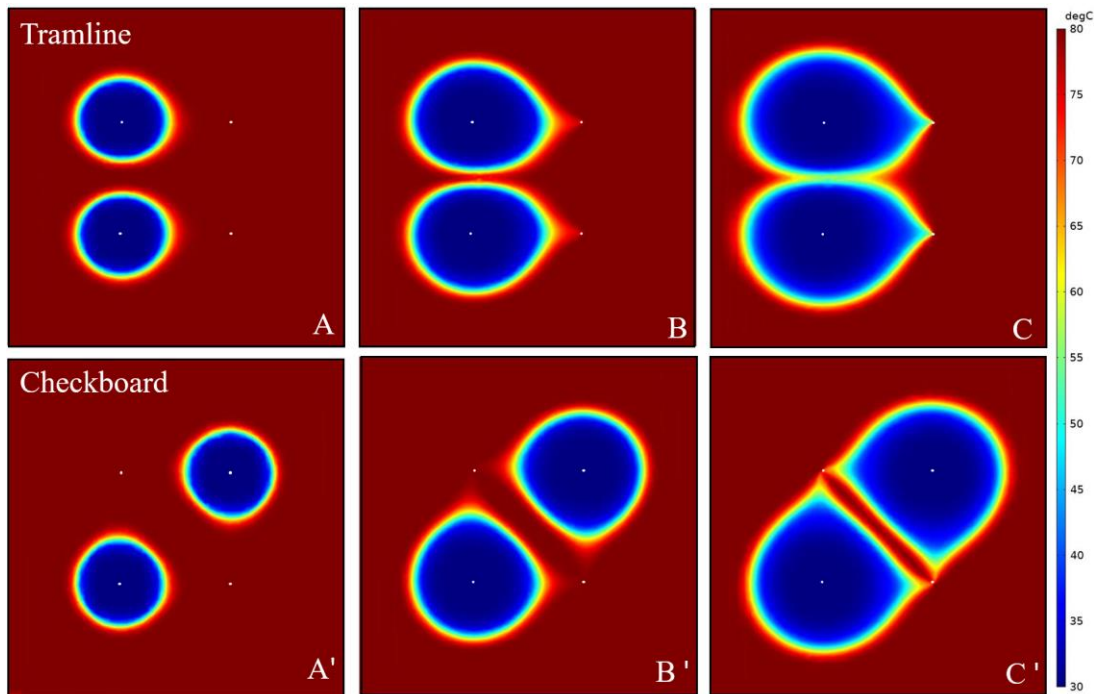


**Figure 6** Development of aquifer temperature for two adjacent single doublets for tramline and checkboard configurations.

Images every ten years of production. A-A'=10years, B-B'=20years and C-C'=30years. Slice at 2500m depth. White dots stand for the wells location.

### 2.1.2 Horizontal well system (Hz-S)

In the case for the horizontal well system, it was set that one single horizontal doublet could replace two single vertical doublets. Therefore, pumping rates were increased to  $Q_{Hz-s1}$ ,  $Q_{Hz-s2}$  and  $Q_{Hz-s3}$  in order to be equivalent with the V-S scenarios. Besides, Well location was varied relatively to the top and bottom boundary of the aquifer (**Figure 7**). It observes in the Hz-S realizations that at low rates and different horizontal length, for instance  $Q_{Hz-s1}$  (**Figure 8a**), production temperature shows an initial plateau in 80°C for at least 15 years ( $L_{Hz1}$ ). Being longer as the  $L_{Hz}$  tends to increase (35 years for  $L_{Hz3}$ ). In addition,  $T_P$  is not deeply affected by the type of wells location in the aquifer (Location 1/2).

**Figure 8** depicts that after the thermal breakthrough temperature declines much faster at high rates, being 2°C/decade for  $Q_{Hz-s1}$  and increasing to 4°C/decade for  $Q_{Hz-s3}$ . In the same way, it is noted that there is a second  $T_P$  “stabilization” which tends to average between the same ranges while the rate is increasing. For instance,  $L_{Hz1}$  after 20 years of production has the same behavior as  $L_{Hz3}$  (See **Figure 8c**), nevertheless there is at least 5 years gap between thermal breakthroughs.

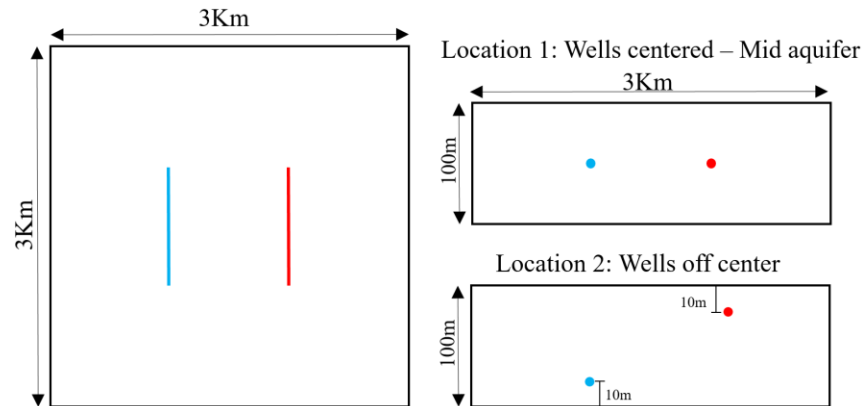


**Figure 7** Schematic layout of Horizontal doublet system configuration. Red stands for producer well and blue for injector well.

Pumping rates play a more important role than horizontal length in terms of production temperature. While rate is increasing, all the curves tend to overlap each other no matter which  $L_{Hz}$  is being used (see **Figure 8a - c**). However, thermal breakthrough gap between  $L_{Hz1}/L_{Hz3}$  does not disappear completely.

On the other hand, while well’s location in the aquifer does not have major effect on temperature declination. In terms of  $\Delta P$ , it plays an important role. **Figure 9** depicts differential pumping pressure and it shows how  $\Delta P$  for Hz-S cases set in Location 2 is higher than in Location

1, having the explanation on the difficulty of injecting cold water (30°C) due to its higher viscosity. As well as the injector well is set in a deeper position, making more visible this effect.

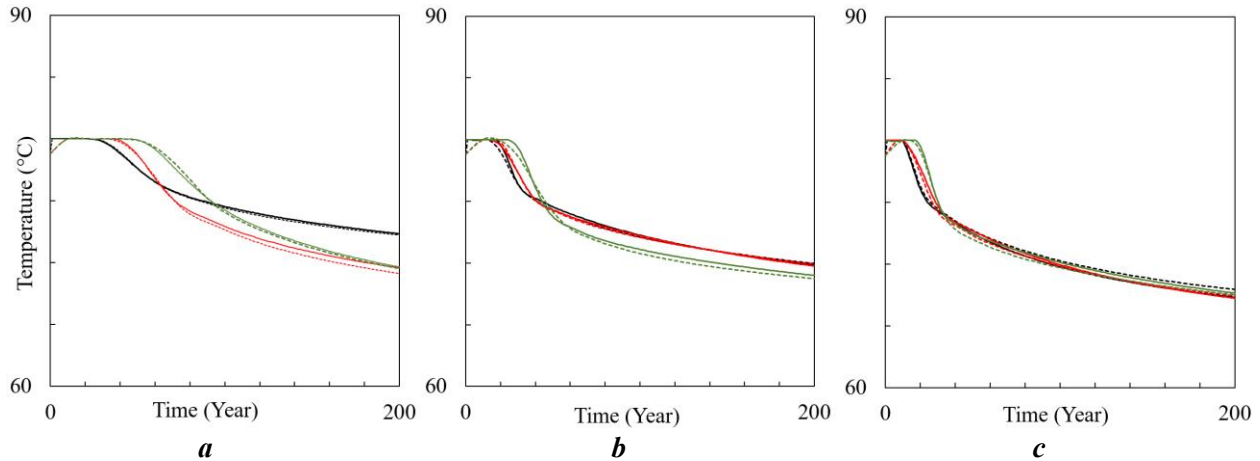


**Figure 8 .** Production temperature profile at different pumping rates).

**a.**  $Q_{Hz-s1}$ , **b.**  $Q_{Hz-s2}$  and **c.**  $Q_{Hz-s3}$ . Black stands for 100m ( $L_{Hz1}$ ), red for 500m ( $L_{Hz2}$ ) and green for 1000m ( $L_{Hz3}$ ). Continues line gives the profile when the wells are set in according to Location 1. Dashed ones when are set in Location 2.

What it can be observed in terms of pressure is that, the longitude of the horizontal well starts to overweigh the effects of increasing pumping rates. While for  $L_{Hz1}$ ,  $\Delta P$  is almost three times larger going from  $Q_{Hz-s1}$  to  $Q_{Hz-s3}$ . For  $L_{Hz3}$ , the increase of  $\Delta P$  is nearly doubled in Location 1 and for Location 2, the increment is not higher than 10%.

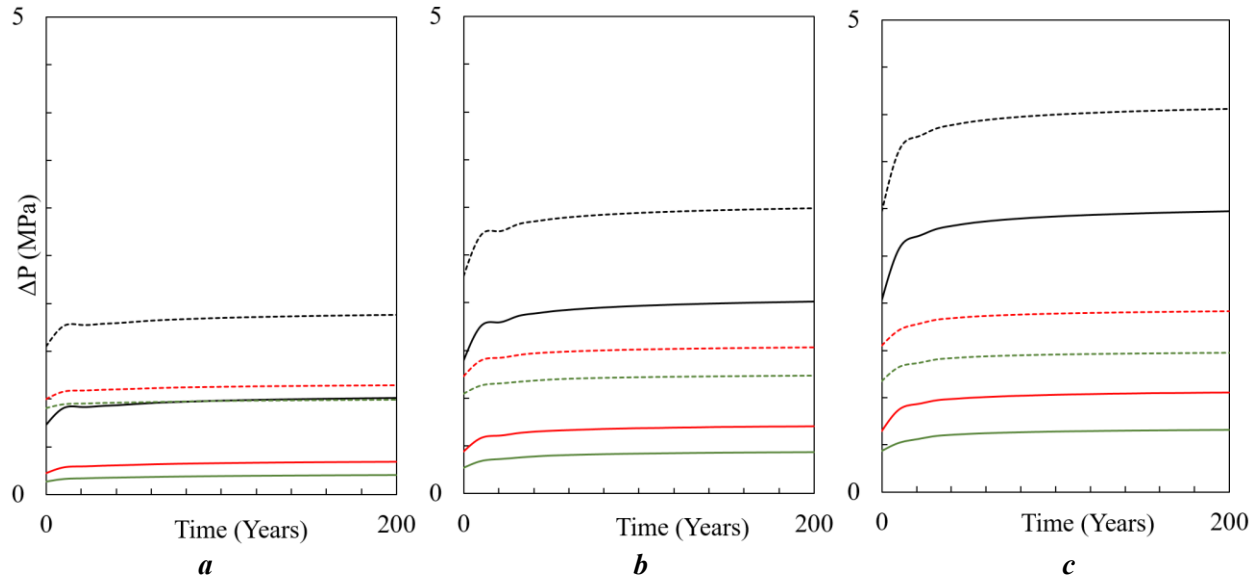


**Figure 9** Differential pumping pressure for Hz-S.

**a.** For  $Q_{Hz-s1}$ , **b.** For  $Q_{Hz-s2}$  and **c.** For  $Q_{Hz-s3}$ . Black stands for 100m ( $L_{Hz1}$ ), red for 500m ( $L_{Hz2}$ ) and green for 1000m ( $L_{Hz3}$ ). Continues line gives the profile when the wells are set in according to Location 1. Dashed ones when are set in Location 2.

### 2.1.3 Comparison V-S to Hz-S

Plots in the **Figure 10** (a, b and c) shows the production temperature profile at different  $Q$  for each Hz-S case compared to the lowest and highest V-S scenarios ( $Q_{V-S1}$  and  $Q_{V-S3}$ , respectively) in both configurations. It depicts that Hz-S scenarios offer better temperature performance even if the thermal breakthrough is reached earlier than in V-S. It notes that the existent thermal breakthrough gap between lowest V-S case and Hz-S tends to be shortened when is coupled L-Hz<sub>3</sub> with  $Q_{Hz-S1}$ . It goes from 30 years of difference to 5 years. Similarly, temperature drop in any Hz-S scenarios has a better performance than the highest V-S ( $Q_{V-S3}$ ), reaching faster the second temperature “stabilization”, which it is a hint of better sweeping of the area from injector towards producer well (See **Figure 11**) at long term.

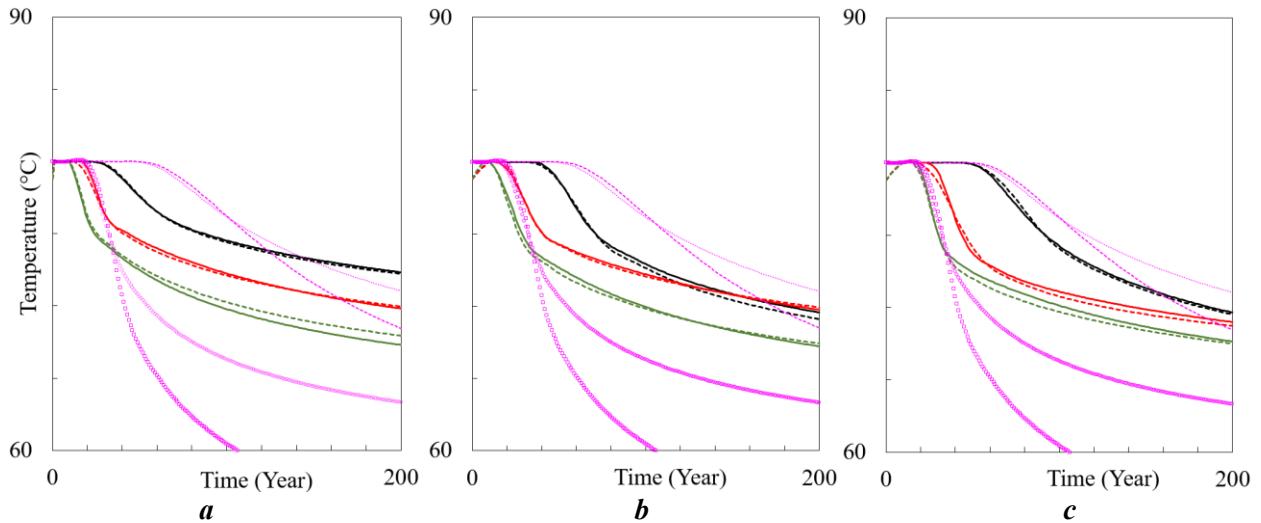


**Figure 10** Comparison of  $T_p$  for Hz-S and V-S.

**a.** For L\_Hz<sub>1</sub>, **b.** For L\_Hz<sub>2</sub> and **c.** For L\_Hz<sub>3</sub>. Dashed and dotted fuchsia lines stand for V-S scenarios ( $Q_{V-S1}$  and  $Q_{V-S3}$ , respectively) in both configurations. Black stands for  $Q_{Hz-S1}$ , red for  $Q_{Hz-S2}$  and green  $Q_{Hz-S3}$  (Solid line represent wells set in Location 1 and dashed one for Location 2).

Since, drilling a long horizontal well and join it to low pumping rates could generate underutilization of the system (L\_Hz<sub>3</sub> and  $Q_{Hz-S1}$ ). For the well spacing used in this study (L=1000m),  $Q_{Hz-S2}$  coupled with any L\_Hz seems to provide the best declination rates after thermal breakthrough and assures that  $T_p$  does not drop below 70°C. Even for L\_Hz<sub>2</sub>, it is comparable with  $Q_{Hz-S1}$  in the long term (**Figure 10b - c**).

In addition,  $Q_{Hz-S3}$  declination rates for any Hz\_S configurations are comparable with the V\_S case of  $Q_{V-S3}$  (Tramline/Checkboard) after thermal breakthrough. Being between 3 and 4°C per decade until it reaches the second stabilization observed in Hz-S cases. Giving the case that,

this rate join to L\_Hz<sub>3</sub> shows better T<sub>P</sub> performance along the whole time than its counterpart in V-S cases (**Figure 10c**).

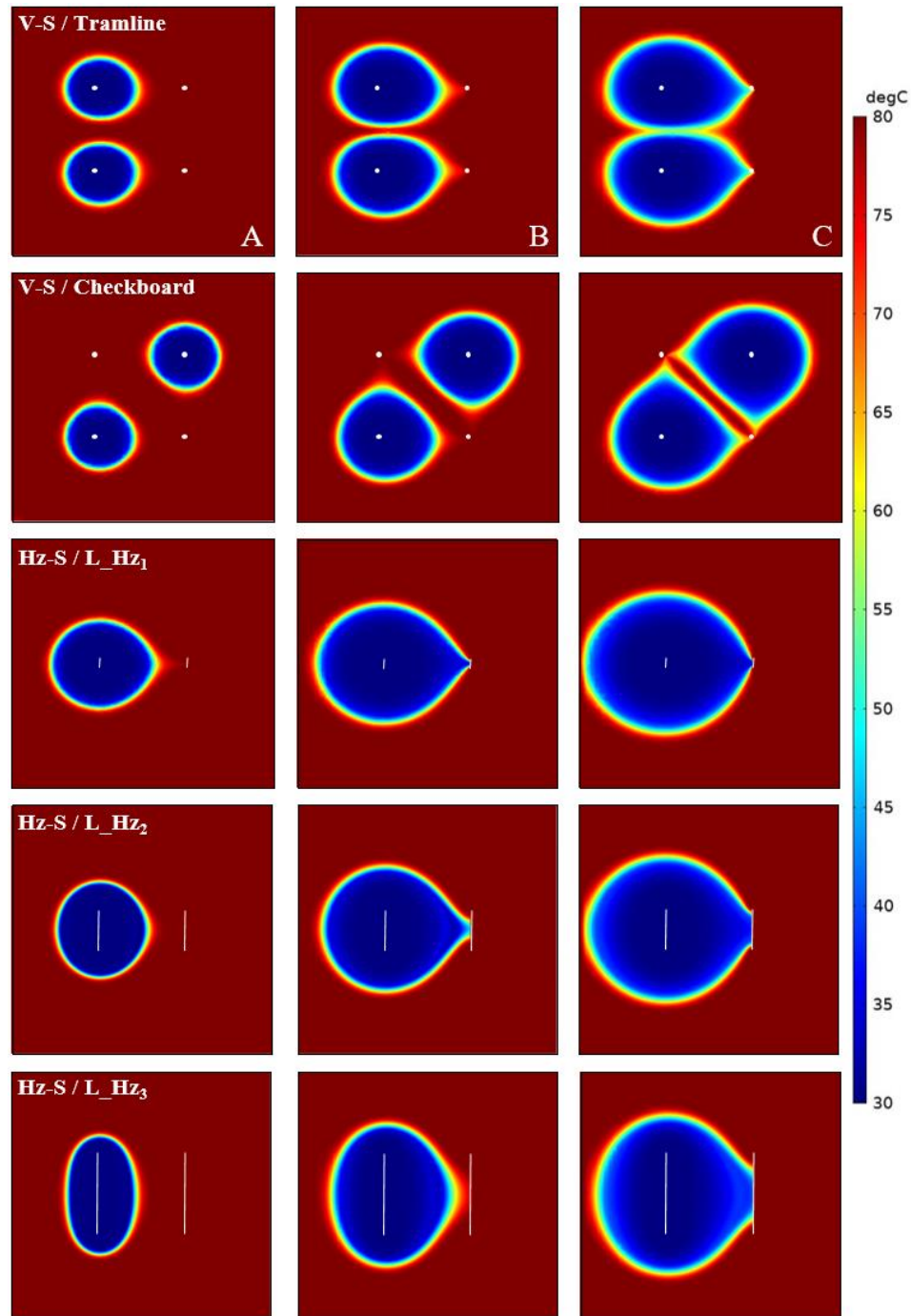


**Figure 11** Temperature plume development for V-S and Hz-S ( $Q_{V-S3}/Q_{Hz-S3}$ ).  
*A=10 years, B=20 years and C=30 years.*

In the same manner,  $\Delta P$  for each Hz\_S scenario is compared with the lowest differential pressure requirements in V-S cases ( $Q_{V-S1}$ , both configurations) and results can be seen in **Figure**

**12.** The improvement in  $\Delta P$  passing from V-S to Hz-S is appreciated as  $L_{Hz}$  increases. Going from four times higher with  $L_{Hz1}$  and  $Q_{Hz-s3}$  (Location 2) than V-S to be barely 50% higher when is set with  $L_{Hz3} / L2$ . Reductions of differential pumping pressure are more noticeable when the wells are in Location 1.

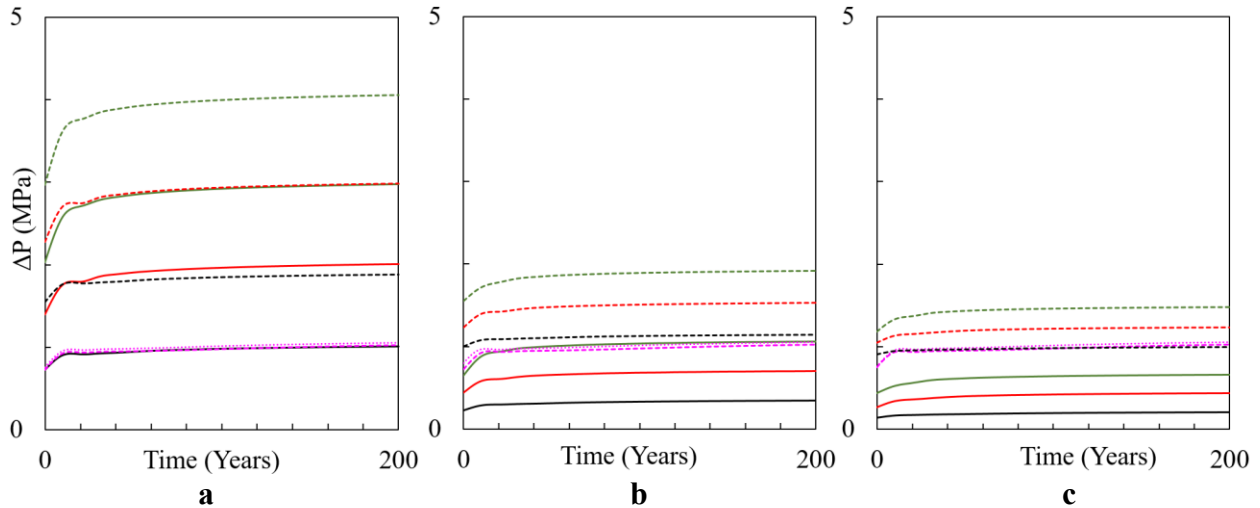


**Figure 12** Differential pumping pressure comparison between V-S and Hz-S.

Fuchsia dashed lines represent V-S of  $Q_{V-s1}$  in tramline and checkboard configurations. **a.**  $L_{Hz1}$ , **b.**  $L_{Hz2}$  and **c.**  $L_{Hz3}$ . Black stands for  $Q_{Hz-s1}$ , red for  $Q_{Hz-s2}$  and green for  $Q_{Hz-s3}$  (Solid line represent wells set in Location 1 and dashed one for Location 2).

As far as it concerns to  $T_P$  and  $\Delta P$ , Hz-S scenarios have shown a better performance than V-S, on the following section this is tested using other key indicators. Which are  $E_{pump}$  (Pump energy losses),  $E_{net}$  (Net energy), COP (Coefficient of performance), S (sweep) and NPV (Net Present Value). **Figure 13** shows the relative difference of the aforementioned indicators for Hz-S respect to the V-S. These parameters were evaluated in two points, when  $T_P$  drops  $1^\circ C$  and  $10^\circ C$  (from here after,  $LT^1$  and  $LT^{10}$ , respectively). Except for the NPV which was accumulated at 15 years of production ( $LT^{15}$ ), since feed-in tariff (SDE +) applies for that period according to the Netherlands regulation [14] [22].

First parameter taken into account is  $E_{pump}$ , which depends on the variation of differential pumping pressure ( $\Delta P$ ). **Figure 13a** depicts that all scenarios in the short term ( $LT^1$ ) are able to reduce or at least keep the same pressure requirements as V-S cases. For instance doublets configured with  $L_{Hz2}$  or  $L_{Hz3}$  reduce the energy losses around 65 and 80% (For all the rates used). While in  $L_{Hz1}$  is observed the same  $\Delta P$  than V-S, either for  $LT^1$  and even in long term ( $LT^{10}$ ). The only exception to this pattern is when doublets are set in Location 2. In the case of  $L_{Hz1}$ , it increases up to an 85% for  $Q_{Hz-s1}$  which it reduced by half (40%) and two-third (35%),

when the systems work with  $Q_{\text{Hz-S2}}$  and  $Q_{\text{Hz-S3}}$ . For lengths  $L_{\text{Hz2}}$  and  $L_{\text{Hz3}}$ , in  $LT^1$  is not seen major improvement. Whereas, at  $LT^{10}$  energy losses is reduced sharply and is more pronounced with high rates, reaching up to 50% ( $Q_{\text{Hz-S3}}$ ).

Next indicator is  $E_{\text{net}}$  that is the difference between energy produced and lost. Most of the Hz-S cases evaluated have a decreased on it. As **Figure 13b** shows, this reduction becomes bigger going from high to low rates. L-Hz<sub>3</sub> coupled with any flow rate are the most frequent Hz-S scenarios that can produced nearly the same amount of net energy than V-S or in some cases more (With  $Q_{\text{Hz-S3}}$ ). In that way, It can be identified a pattern where the combination  $L_{\text{Hz3}}$  with  $Q_{\text{Hz-S3}}$  at Location 2 always obtained more  $E_{\text{net}}$  than any V-S in checkboard configuration for the long term ( $LT^{10}$ ). Which is coherent with what was seen in the previous **Figure 10c**.

Coefficient of performance, COP, is defined as the ratio between produced energy and energy losses. At first sight of **Figure 13c**, it is possible to identify that for  $L_{\text{Hz2}}$  and  $L_{\text{Hz3}}$  set in Location 1 give a huge improvement of unit energy produced by unit lost against any V-S configuration (Around 200 and 400%, respectively) for both  $LT^1$  and  $LT^{10}$ . It can be assumed that acts as sort of “zoom” of what was seen in the lower part of **Figure 13a**. Meanwhile, COP for Hz-S cases in Location 2 tend to improve while horizontal length and pumping rate are increasing. Thus,  $L_{\text{Hz2}}$  and  $L_{\text{Hz3}}$  present a more pronounced slope than  $L_{\text{Hz1}}$ . Besides this horizontal length at Location 1 does not offer any variation, it is nearly similar to V-S.

Even with the better COP performance for Hz-S observed, in the short term ( $LT^1$ ). **Figure 13d** depicts a worsening for most of cases in the Sweep (S) indicator, which refer to the ratio of produced energy and total energy of the reservoir. Whereas, at  $LT^{10}$  it sees the major enhance in sweep is given by Hz-S doublets set either Location 1 or 2 at the high rates compared to their counterpart in V-S cases. That performance is dictated by the “stabilization” in  $T_p$  after thermal breakthrough, which was observed in **Figure 10**.

**Figure 14** shows the las two indicators evaluated. Lifetime of the system was weighed at  $LT^1$  and  $LT^{10}$ . It observed that the  $LT^1$  for all rates used coupled with  $L_{\text{Hz21}}$  or  $L_{\text{Hz22}}$  (Location 1) is reduced between 40 and 50%, respectively. While, the longest longitude  $L_{\text{Hz3}}$  (both Location 1 or 2) keeps the advance of cold water similar to what was obtained for V-S.  $LT^{10}$  values depict once again that Hz-S configurations give a better performance in the long term than V-S. Mostly, when the systems are set as Location 2 for high rates at any  $L_{\text{Hz}}$ .

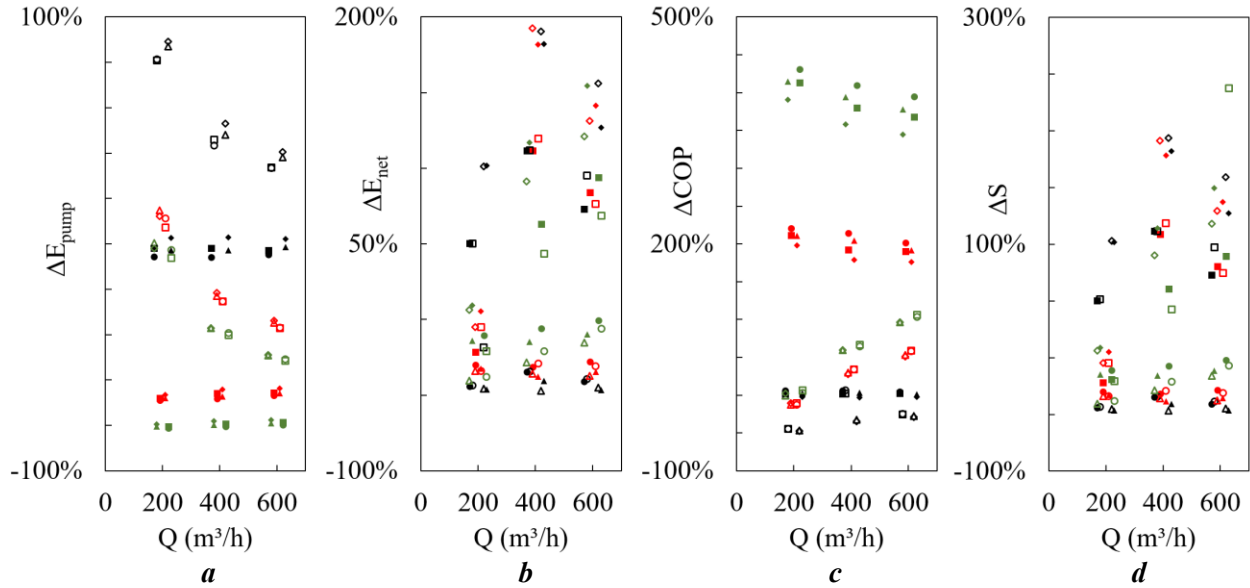


**Figure 13** Key parameters comparison between V-S and Hz-S.

**a.**  $E_{pump}$ , **b.**  $E_{net}$ , **c.** COP and **d.** Sweep. At  $LT^1$ , Circles is  $V\_S$  tramline compared to  $Hz\_S$  and triangles is  $V\_S$  checkboard compared to  $Hz\_S$ . At  $LT^{10}$ , squares is  $V\_S$  tramline compared to  $Hz\_S$  and rhombus is  $V\_S$  checkboard compared to  $Hz\_S$ . Filled shapes represent comparison to  $Hz\_S/L1$  while empty shapes are for comparing to  $Hz\_S/L2$ . Black stands for  $L\_Hz_1$ , red for  $L\_Hz_2$  and green for  $1000m L\_Hz_3$ .

Finally, knowing that there are some drawbacks about Hz-S configurations as heat exploitation strategy. Mostly related to  $L\_Hz_1$  that in terms of aforementioned parameters, it has a very low impact (Location 1) or in some cases showing a lower performance (Location 2). When NPV indicator is taken into account. Any horizontal length combined with any pumping rate set in this study have shown the beneficial effect of replacing V-S for Hz-S. As it see in **Figure 14** for the case of  $L\_Hz_1$ , its drawbacks are compensated with an increment of NPV up to eight times at low rates ( $Q_{Hz-S1}$ ), which decreases as pumping rate is increasing. It perceived that coupling  $Q_{Hz-S3}$  with most of  $L\_Hz$ ,  $\Delta NPV$  tends to concentrate in an increment of 10% respect to V-S. Lastly,  $Q_{Hz-S2}$  offers a wider variability of NPV in function of  $L\_Hz$ . Going from 40% for the shortest length to 60% for longest one.

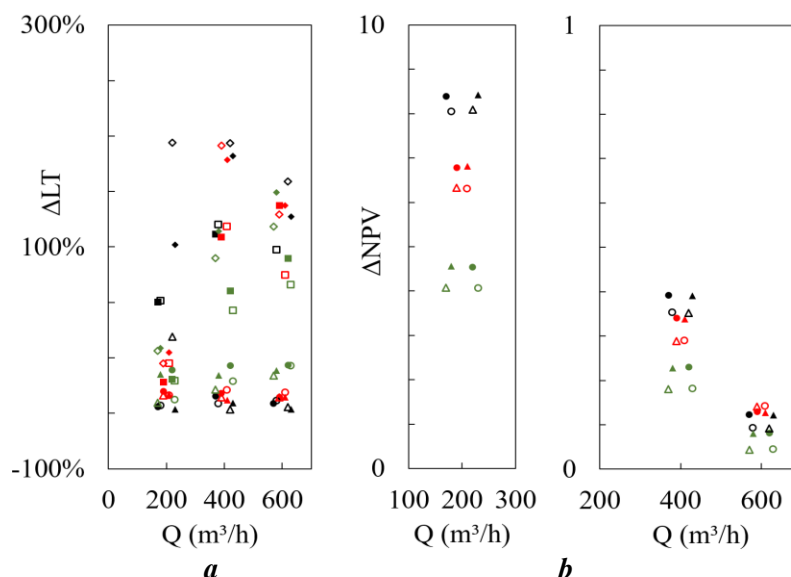


**Figure 14** Key parameters comparison between V-S and Hz-S, second part.

**a.** LT and **b.** NPV. At  $LT^I$ , Circles is  $V\_S$  tramline compared to Hz\_S and triangles is  $V\_S$  checkboard compared to Hz\_S. At  $LT^{I0}$ , squares is  $V\_S$  tramline compared to Hz\_S and rhombus is  $V\_S$  checkboard compared to Hz\_S. NPV is compared at 15 years. Filled shapes represent comparison to Hz\_S/L1 while empty shapes are for comparing to Hz\_S/L2. Black stands for  $L\_Hz_1$ , red for  $L\_Hz_2$  and green for 1000m  $L\_Hz_3$ .

#### 2.1.4 Comparison Hz-S to MLT-S

The current study was also performed to get insights about the use of multilateral wells as development strategy instead of horizontal wells (and/or vertical). More specifically, the Radial Jet Drilling (RJD) technology. **Figure 15** shows the performance of MLT-S against to the others two system already evaluated for a pumping rate of  $200\text{m}^3/\text{h}$  ( $Q_{\text{MLT-S}}$ ). In terms of temperature development, it presents similar behavior to V-S (checkboard configuration), even the thermal breakthrough is delayed around one year. It can be infer that the laterals added to the vertical well do not shorten the well spacing. From these outcomes, it would be expected that the temperature plume shape should have analogous behavior to the V-S, which it can be appreciated in the **Figure 16****Error! Reference source not found.**, a teardrop shape becoming asymmetrical in two directions while cold water gets closer to the producer wells. Nevertheless, it does not present the second “stabilization” in  $T_p$  compared to Hz-S. On the other hand,  $\Delta P$  is greatly improved (See **Figure 15b**). Compare to its counterpart in V-S and for the case of Hz-S in Location 1 for  $L\_Hz_1$ , it is reduced around 60%. For Location 2 with the same  $L\_Hz$ , the enhancement is more pronounced which is up to 80%. Such as it is the improvement that can be comparable with the pressure requirements for  $L\_Hz_2$ .

In order to evaluate the key indicators seen before. It was calculated the relative difference of Hz-S (And V-S) cases against MLT-S, which are summarize in the **Figure 17**. Which show that MLT-S indicators have a similar performance to V-S in most of the indicators estimated. Only parameters like COP and NPV, it can be seen important variations. COP for V-S is being reduce more than 50%, no matter configuration pattern (Tramline/Checkboard) set. This is mainly, because energy losses have been decreased substantially (Lower  $\Delta P$  – Presence of Laterals). Seeing NPV, it is increased about 30% due to the increment of initial investment for RJD technology and the annually operational costs related to it.

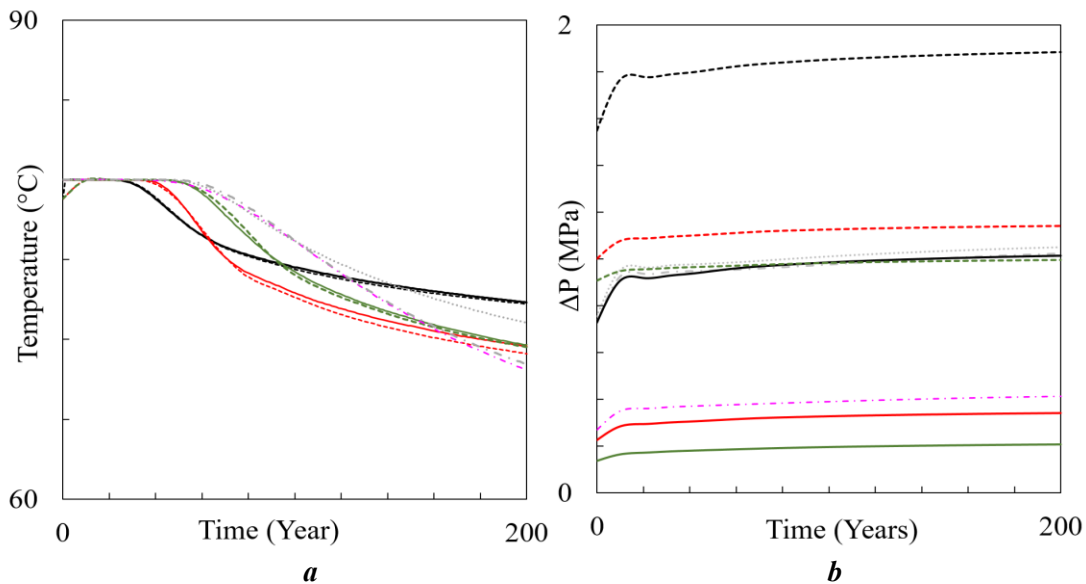


**Figure 15** Temperature and differential pumping pressure profiles at 200m<sup>3</sup>/h. Black stands for L\_Hz1, red for L\_Hz2 and green for 1000m L\_Hz3. Dashed fuchsia line stands for MLT-S. Grey line stands for V-S (Tramline and Checkboard)

On the other hand, when MLT-S is compared to Hz-S. Only long horizontal sections (L\_Hz<sub>1</sub> /L\_Hz<sub>1</sub>) set in Location 1 provide lower energy losses, for the rest of cases MLT-S allows an enhancement of 150%, either short or long term (**Figure 17a**). Analogous pattern is observed for COP, where aforementioned lengths provide a better performance, only at LT<sup>1</sup>. As production advances, MLT-S is improved more than 50% (**Figure 17c**).

All the scenarios present a worst performance in LT<sup>1</sup> compared to MLT-S in the case of net energy. Only scenarios like L-Hz<sub>1</sub> (Either Location 1 or 2) and V-S in tramline configuration are capable of providing higher amounts of energy and jut apply at LT<sup>10</sup>. Given by the slow advance of cold water, in V-S generating soft declination rates and Hz-S thanks to a long temperature stabilization after thermal breakthrough (See **Figure 15a**). In terms of NPV, Hz-S is still offering

a much better performance. However, the increment is less pronounced. Around 6 times for the shortest  $L\_Hz$  evaluated (Instead of 8 times compared to V-S). **Figure 17** confirms once again that, Hz-S in Location 1 provides a faster return of initial investment. Mainly, given for advantage on  $\Delta P$  that has over Location 2.

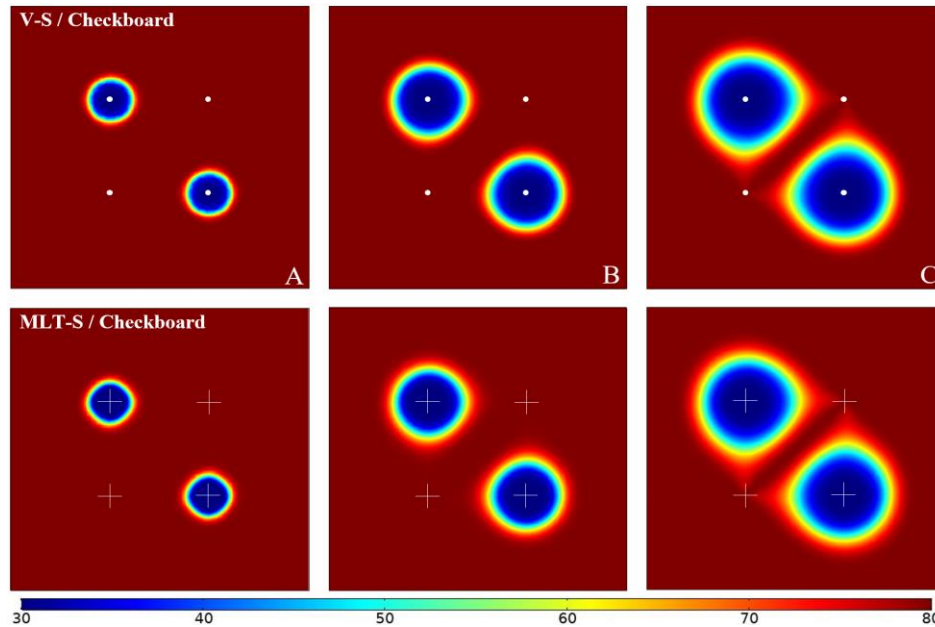


**Figure 16** Temperature plume development ( $^{\circ}\text{C}$ ) for V-S and MLT-S with a pumping rate of  $100\text{ m}^3/\text{h}$  per well.  $A = 10$  years,  $B = 30$  years and  $C = 60$  years.

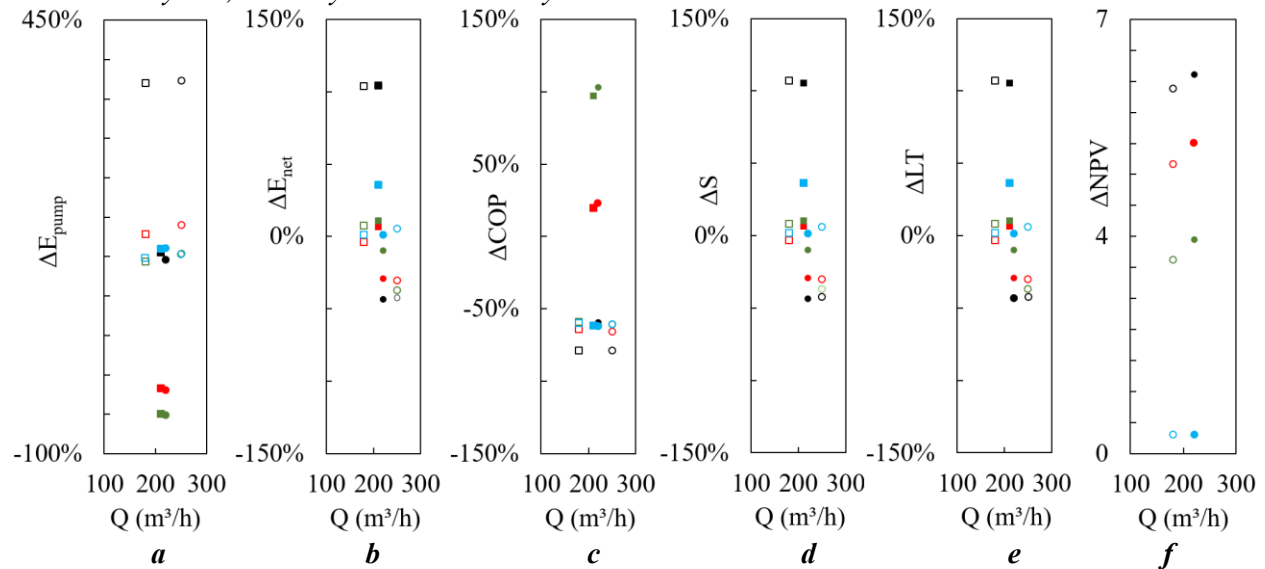


**Figure 17** Key parameters comparison between Hz-S (V-S) and MLT-S-S at  $200\text{ m}^3/\text{h}$ .

**a.**  $E_{\text{pump}}$ , **b.**  $E_{\text{net}}$ , **c.** COP, **d.** Sweep, **e.** LT and **f.** NPV. Circles stand for  $LT^1$  while squares for  $LT^0$ . Filled shapes represent difference against Hz-S scenarios in Location 1 while empty shapes are for Location 2. Black stands for  $L\_Hz_1$ , red for  $L\_Hz_2$  and green for  $1000\text{ m } L\_Hz_3$ . Blue color stands for V-S, where filled shape relates to Tramline configuration and empty one for Checkboard. NPV (f) was accumulated after 15 years of production.

## 2.2 Heterogeneous Model

Following sections will be found the outcomes related to sensitivities done over the three different heterogeneous systems. In order to determine the impact of heterogeneity over the type of system used and vice versa.

### 2.2.1 Heterogeneity – $k_1$

This model was tested with three different scenarios which are:

- ❖ V-S in checkboard configuration ( $Q_{V-S3}$ ).
- ❖ Hz-S for L-Hz<sub>2</sub> in Location 1 ( $Q_{Hz-S3}$ ).
- ❖ MLT-S in checkboard configuration with a pumping rate of 300m<sup>3</sup>/h per well.

In this model where the degree of heterogeneity is low (Variance of 0.04). The scenarios tested tend to behave as the homogenous one. Since, it can see the similar temperature profile in V-S and MLT-S configurations (**Figure 18a**). Having similar thermal breakthrough time, the development of cold water front seems to be accelerated near to the producer because of laterals in MLT-S (**Figure 19**), reason by which the declination rate is stronger in this system (Around 2°C/decade more than V-S).

In term of Hz-S, the absence of a second adjacent doublet generates that the declination in temperature after breakthrough not last more than 10 years and the  $T_P$  drop is from 80°C to 70°C. Even though, cold-water front breaks into the producer well very early (Close to after 3 years of production – **Figure 19**). Which for V-S and MLT-S takes up to 15 years before seeing the second “stabilization” and it drops around 20°C. It seems that the surrounding area is able to keep warmer the water going-in for the case Hz-S when are set in Location 1. Also, the producer well is being affected just from one direction instead of 2 that is the case for V-S/MLT-S. In addition, Differential pumping pressure is highly decreased either in Hz-S and MLT-S as it was seen in homogenous realizations, nearly in the same proportion. Hz-S provides a more steady temperature profile and lower pressure requirements with a single doublet along of the whole simulation time.

Nevertheless, at  $LT^1$  and  $LT^{10}$ , which are the crucial point of evaluation of the systems. Thermal breakthrough and lifetime for V-S and MLT-S are delayed 12 and 7 years, respectively. While Hz-S tends to compensate this disadvantage with the big enhancement of  $\Delta P$ . Being, extremely high compared to the conventional system and at least 25% less than MLT-S.

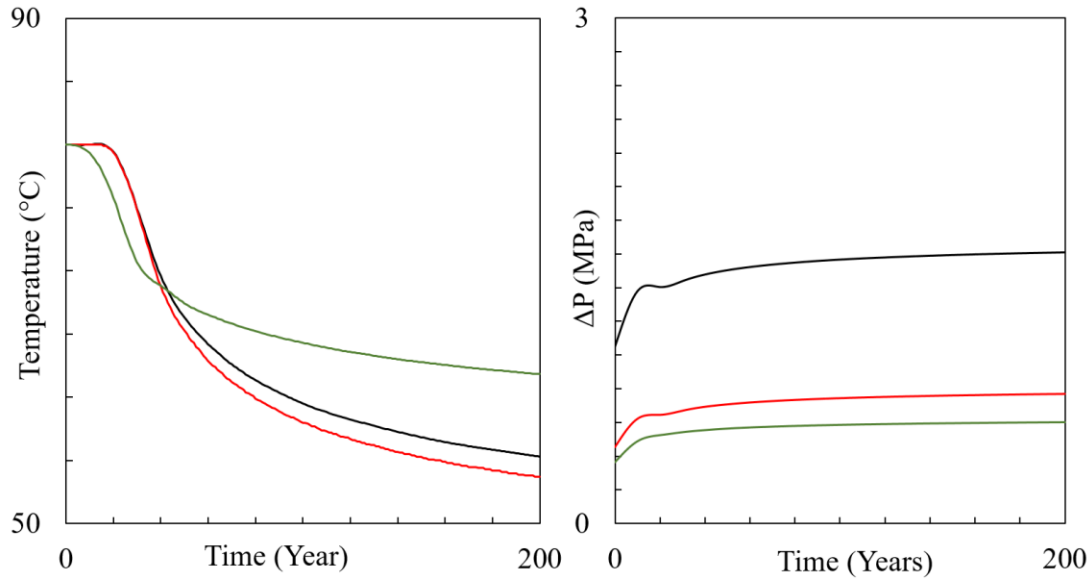


**Figure 18** Temperature and differential pumping pressure for different systems in  $k_1$ . Black line stands for V-S set with  $Q_{V-S3}$ , Red lines for MLT-S ( $300\text{m}^3/\text{h}$ ) and green ones for Hz-S set with  $L\_Hz_2$  (Location 1) and  $Q_{Hz-S3}$ .

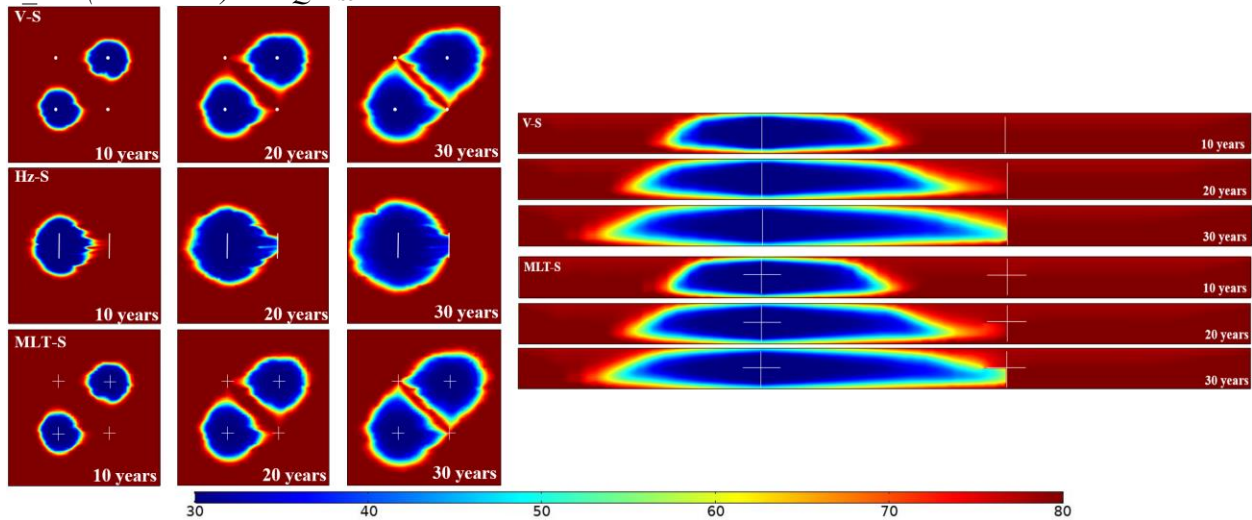


**Figure 19** Temperature development during 30 years for V-S, Hz-S ( $L\_Hz_2$  – Location 1) and MLT-S for a total pumping rate of  $600\text{m}^3/\text{h}$  in  $k_1$ .

**a.** Top view **b.** Lateral view for V-S and MLT-S.

### 2.2.2 Heterogeneity – $k_2$

In the case of the second heterogeneity model, which is the highly anisotropic. The sensitivities conducted for  $k_1$  plus a realizations with L-Hz<sub>3</sub> in Location 2 and applying constant pressure boundaries for MLT-S configuration were performed to evaluate the impact of the system in  $k_2$ .

System  $k_2$  gives the opportunity to take a look at how the doublet location generates a preferential path flows, in function of the heterogeneity. Firstly, **Figure 20** shows temperature and

pressure profiles for each configuration tested. V-S and MLT-S have comparable  $T_P$  until the thermal breakthrough has been reached (**Figure 20a**). It confirms that the laterals presence in the well contribute to a faster decline, as it was seen in  $k_1$  (Being even more pronounced in this case –  $k_2$ ). Respect to the Hz-S evaluated, temperature pattern in which thermal breakthrough is reached faster as  $L_{Hz}$  increases, it has been shifted in the current case.  $L_{Hz_3}$  in Location 2 has given better performance than  $L_{Hz_2}$  in Location 1 (Both for  $Q_{Hz-S_3}$ ). Thermal breakthrough was delayed for about 5 years and the system kept  $T_P$  above  $65^\circ\text{C}$  while for the other combination it was reduced to  $60^\circ\text{C}$ . Talking about  $\Delta P$  (**Figure 20b**), MLT-S is the configuration capable of maintaining very low pressure requirements while increasing permeability variation. It can be comparable with other system only if this is an Hz-S set with longer horizontal sections.

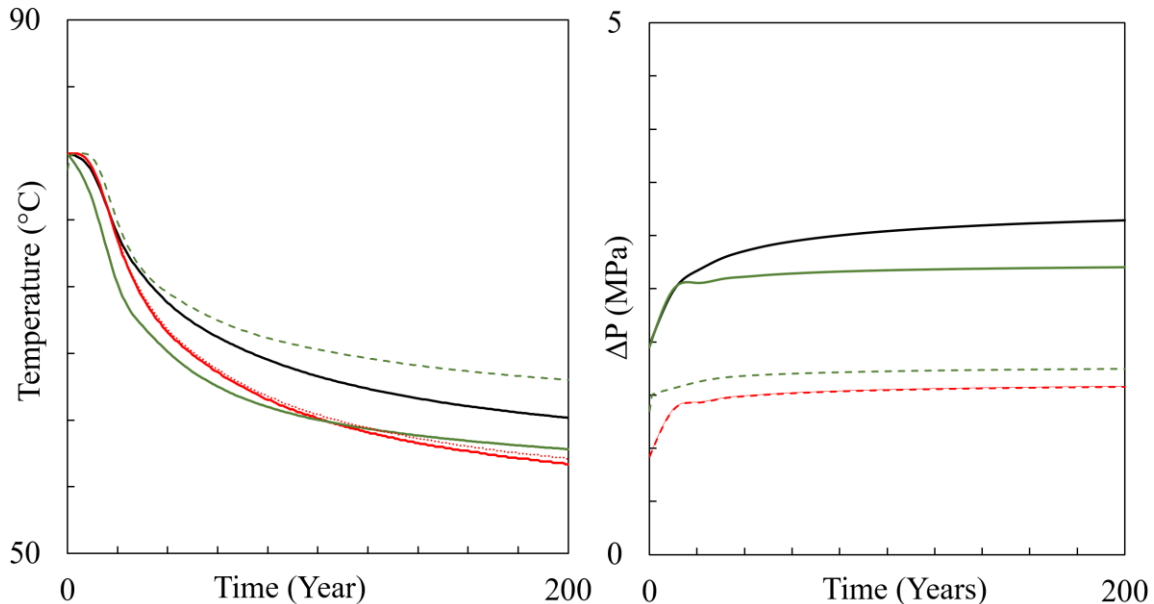


**Figure 20** Temperature and Pressure profile for different systems in  $k_2$ .

Black line stands for V-S set with  $Q_{v-s_3}$ , Red lines for MLT-S ( $300\text{m}^3/\text{h}$ ), green continuous lines for Hz-S set with  $L_{Hz_2}$  (Location 1 -  $Q_{Hz-S_3}$ ) and dashed green ones for Hz-S set with  $L_{Hz_3}$  (Location 2 -  $Q_{Hz-S_3}$ )

By **Figure 21**, it can be appreciated how preferential paths are generated. While in V-S and MLT-S, cold water front follows the highest permeability channel. The advance of the front in Hz-S is more uniformly distributed along the horizontal section as  $L_{Hz}$  increases until it is reached those paths. However, It is also seen how cold-water tends to look for these permeable paths at early stages in Hz-S.  $L_{Hz_2}$  depicts this pattern, when at very early production stages it has already connected both wells through one of these channels. Reason by which in **Figure 20a**. is not seen the expected plateau before thermal breakthrough.

### 2.2.3 Heterogeneity – $k_3$

This model represents a variation of  $k_2$ , since it has been kept same parameter for its generation except for the direction of the channels, which were inclined 45 degrees. In order to evaluate the impact of doublet location with respect to the main flow direction. All three systems were tested, checkboard for V-S/MLT-S and L\_Hz<sub>2</sub> (Location 1) for Hz-S. They were set with a total pumping rate of 600m<sup>3</sup>/h.

In terms of development temperature, all systems show an improvement (See **Figure 22**). Thermal breakthrough is delayed 5 years for Hz-S and 10 year in the other two, with respect to what was seen in  $k_2$  model. It is an indicative that cold-water flow was not directed in early stages towards the producer well even though there is existence of 2000-3000mD channels (**Figure 4c**). After breakthrough, all systems present the same pattern seen in homogenous and the other two heterogeneity realizations. Being a better performance in case of Hz-S and a faster declination for MLT-S.

Where it can be seen the major variations respect to  $k_2$  is when  $\Delta P$  is taken into account. Firstly, it has been increased in about one order of magnitude. Where, V-S was more affected and, also Hz-S were influenced by this channels configuration/direction. Because the surrounding areas of either vertical well or any part of the horizontal section, the continuity of permeable channels is not uniform (As it seen in  $k_2$ ). Reason why, it is observed how  $\Delta P$  increased very quickly in initial stages of simulation time (Earlier than 15 years) and then tends to slowly decrease and stabilize, when the main flow paths have been reached (See **Figure 23**). Acknowledging this, MLT-S has shown a performance more closely to what would be expected for  $\Delta P$ , initial increased of it up to reach a plateau. Finding, its reason on the fact that laterals increase the probability that the wells could contact permeable channels and keeping more stable pressure requirements.

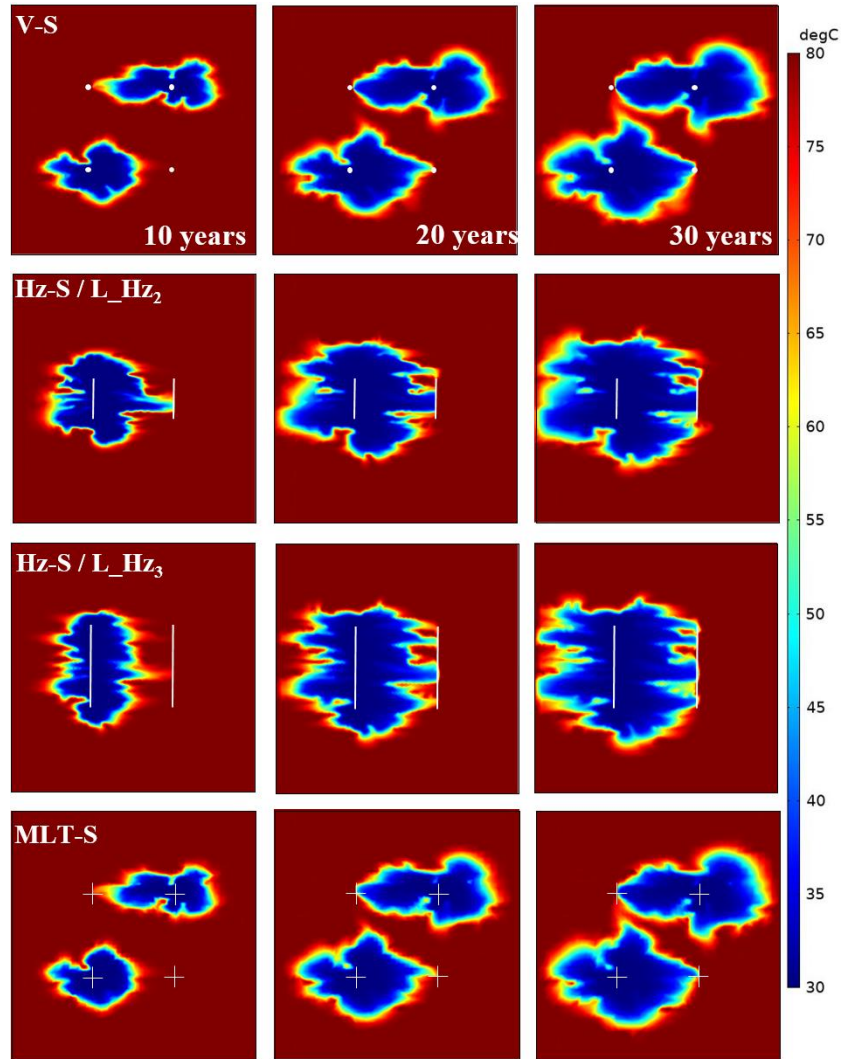


**Figure 21** Temperature development during 30 years for V-S, Hz-S ( $L_{Hz_2} - L_{Hz_3}$ ) and MLT-S for a total pumping rate of  $600\text{m}^3/\text{h}$  in  $k_2$ .

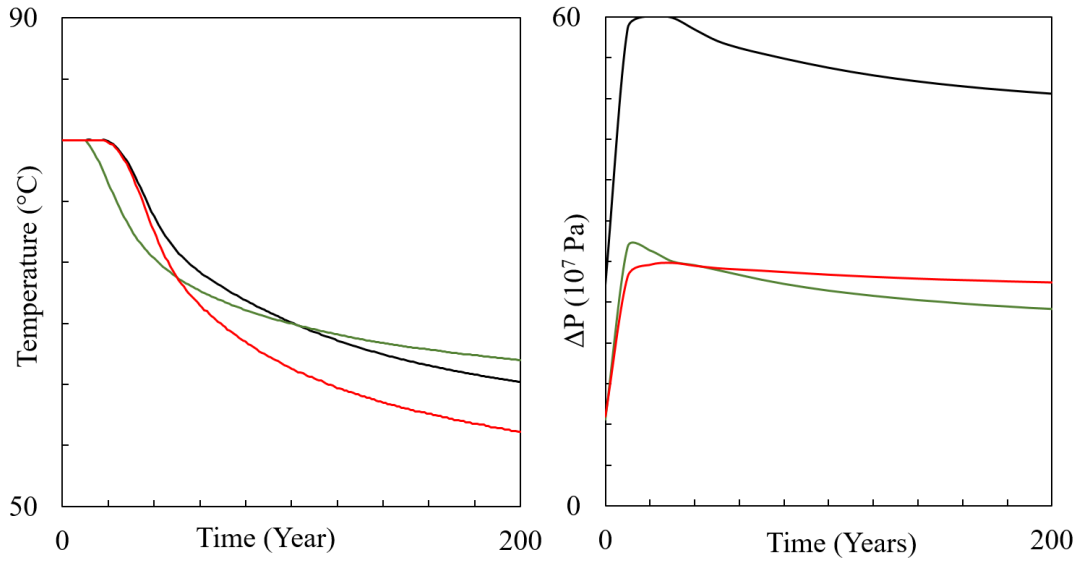


**Figure 22** Temperature and differential pumping pressure for different systems in  $k_3$ . Black line stands for V-S set with  $Q_{V-S3}$ , Red lines for MLT-S ( $300\text{m}^3/\text{h}$ ) and green ones for Hz-S set with  $L_{Hz2}$  (Location 1) and  $Q_{Hz-S3}$ .

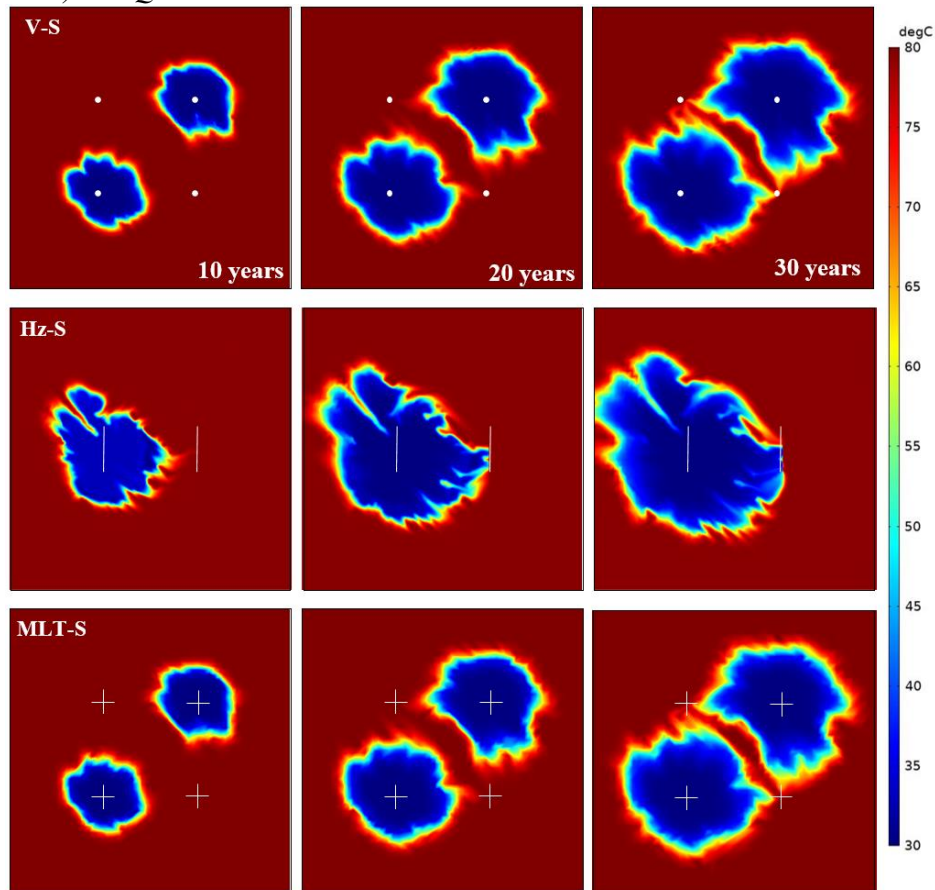


**Figure 23** Temperature development during 30 years for V-S, Hz-S ( $L_{Hz2}$  – Location 1) and MLT-S for a total pumping rate of  $600\text{m}^3/\text{h}$  in  $k_2$ .

### 3. CONCLUSIONS

The current study presented different advantages and disadvantages related to geothermal doublets performance using vertical, horizontal and/multilateral wells as part of it. It has been demonstrated that for the well spacing used here. Thermal breakthrough in V-S configurations always is delayed compared to Hz-S between 8 to 10 years at low rates and from 2 to 4 years with high rates. While, temperature declination rates are softer for the case of horizontal wells configurations after the breakthrough. Therefore, looking at  $LT^1$  (short term), most of the lifetime in Hz-S are reduced as much as 40%, this percentage is reduced as flow rates and horizontal length increase, to 10%. On the other hand, at  $LT^{10}$  it was seen the great impact of Hz-S, enlarging the lifetime for more than 40 years when the system works at high rates (400-600m<sup>3</sup>/h). In addition, Hz-S continues showing its impact when is about pressure requirements. Longer horizontal lengths ( $L_{Hz2}$  and  $L_{Hz3}$ ) have provide reductions for at least 40%. Nevertheless, it was seen some drawbacks for Hz-S with short  $L_{Hz}$ , where there was no change with respect to V-S or in some cases (at Location 2) showing a worst performance, given by the hardness of injecting cold water when depth increases (Viscosity matters).

Among of the five key indicators ( $E_{pump}$ ,  $E_{net}$ , COP, Sweep and NPV) evaluated, V-S just can overweigh Hz-S in two of them and only at short term. Which are net energy produced and sweep, until 50% better for V-S. All this giving by the fact that thermal breakthrough in Hz-S is reached earlier. At the long term, Hz-S reaches until 200% of enhancement in those two indicators, when the wells are located in the middle of the aquifer. On the other hand, only when  $L_{Hz}$  is very short, energy losses have not reduced. For the other cases, the improvement has varied between 20 to 80%. Where at short term it is observed the major boost of  $E_{pump}$ , while in the long term, it is seen progressively with the increment of horizontal length and pumping rates, reaching until 60% of reduction. Such is the boost generated by Hz-S about  $\Delta P$  that the COP has shown an increment of almost 400% for long  $L_{Hz}$  at  $LT^1$  or 100% at  $LT^{10}$  with any rate tested.

It has been demonstrated that not only  $E_{pump}$  has been highly reduced, COP is boosted in any of location used (Location 1/2) and  $E_{net}$ , sweep and lifetime are enhanced at long term. But also, NPV confirms all these technical benefits observed of using Hz-S as development configuration. Even, looking at  $L_{Hz1}$ , which was the worst technical scenario, the NPV differences respect to V-S reached extremely high values (8 times higher) or taking into account

the most expensive Hz-S scenario,  $L_{Hz3}$  coupled with  $Q_{Hz-S3}$ , it still observed a growth of 8 to 10% compared to its counterpart in V-S.

Besides, it has been showed that comparing Hz-S to MLT-S has similar pattern than comparing to V-S, for most of the key indicators. Major differences can be found in  $\Delta P$ , for MLT-S can be comparable with all Hz-S in Location 2 and some cases better ( $L_{Hz1}$ ). Just at large  $L_{Hz}$ , Hz-S offers better behavior, which coupled with low flow rates can be an overdesigned system. However, once again NPV dictated an important difference between systems. Which for the longest length is still offering a four times increment.

Once heterogeneity is accounted, what was identified is that depending on the grade of anisotropy (Low= $k_1$  and High= $k_2$ ), connectivity between injector and producer wells could be increased. Which generate early thermal breakthrough and therefore shortening the lifetime of the system, case of  $k_2$ . The fact of locating the doublets in a way that do not have direct connection paths ( $k_3$ ), allows to enlarge the lifetime of the doublet in any system up to 10 years. Whereas,  $\Delta P$  is highly affected. Mostly for vertical systems, since the surrounding areas do not offer a constant permeability paths. That in the case of Hz-S and MLT-S is faced by the longitude of the horizontal section and the laterals providing connection with different permeable bodies, respectively.

This study have allowed to identify that Hz-S overweighs both V-S and MLT-S. Either decreasing energy losses or increasing COP in a short term and/or increasing net energy and NPV in the long term. Reason why, it would be worth to expand this study in terms of deepening in the relation between well spacing and length of horizontal section. And, also an optimization over laterals direction in MLT-S would be important to evaluate and determine if that is capable of counterbalance the existence differences between systems.

## References

- [1] Heekeren, Van, The Netherlands Country Update on Geothermal Energy., Netherland: World Geothermal Congress, 2015.
- [2] D. Bonté, J. Van Wees, -D and J. Verweij, "Subsurface temperature of the onshore Netherlands: new temperature dataset and Modeling.," *Netherlands Journal of Geosciences - Geologie En Mijnbouw*, pp. 491-515, 91 (04).
- [3] R. Ma and C. Zheng, "Effects of density and viscosity in modelling heat as a groundwater tracer," *Ground water*, vol. 48 (3), no. 2010, pp. 380-390, 2010.
- [4] S. Saeid , R. Al-Khoury, H. Nick and F. Barends, "Experimental-numerical study of heat flow in deep low-enthalpy geothermal conditions.," *Renewable Energy*, vol. 62, no. February 2014, pp. 716-730, 2014.
- [5] D. Mottaghy, R. Peching and C. Vogt, "The geothermal project Den Haag: 3D numerical models for temperature prediction and reservoir simulation," *Geothermics*, vol. 40, no. September 2011, pp. 199-210, 2011.
- [6] C. Vogt , S. Iwanowski, G. Marquart, J. Arnold, D. Mottaghy, R. Peching, D. Gnjesda and C. Clauser, "Modeling contribution to risk assessment of thermal production power for geothermal reservoirs," *Renewable Energy*, vol. 53, no. May 2013, pp. 230-241, 2013.
- [7] A. Franco and M. Vaccaro, "Numerical simulation of geothermal reservoirs for the sustainable design of energy plants: A review," *Renewable and Sustainable Energy Reviews*, vol. 30, no. February 2014, pp. 987-1002, 2014.

- [8] G. Madhur, B. Anderson and B. Anderson, "Sensitivity Analysis of Low-Temperature Geothermal Reservoirs: Effect of Reservoir Parameters on the Direct Use of Geothermal Energy," *GRC Transactions*, vol. 36, no. 2012, pp. 1255-1262, 2012.
- [9] J. Sippel, S. Fuchs, M. Cacace, A. Braatz, O. Kastner, E. Huenges and M. Scheck-Wenderoth, "Deep 3D thermal modelling for the city of Berlin (Germany)," *Environmental Earth Sciences*, vol. 70, no. 8, pp. 3545-3566, 2012.
- [10] S. Sanaz, A.-K. Rafid, N. M. Hamidreza and H. A. Micheal, "A Prototype design model for deep low-enthalpy hydrothermal systems," *Renewable Energy*, vol. 77, no. January 2015, pp. 408-422, 2015.
- [11] H. Mijnlief and J. Van Wees, "Rapportage ruimtelijke ordening geothermie.," TNO, Utrecht, 2009.
- [12] J. W. Cees, M. N. Hamidreza, J. W. Gert and F. B. David , "An evaluation of interferences in heat production from low enthalpy geothermal doublets systems," *Elsevier*, vol. 135, no. 135, pp. 500-512, 2017.
- [13] R. Croojimans, C. Willems, H. Nick and D. Bruhn, "The influence of facies heterogeneity on the doublet performance in low enthalpy geothermal sedimentary reservoirs," *Elsevier - Geothermics*, vol. 64, no. November 2016, pp. 209-219, 2016.
- [14] NLOG, "<https://www.nlog.nl/en>," NLOG, Ntherlands, 2019.
- [15] J. W. Cees, M. N. Hamidreza, E. D. Marinus, W. Gert Jan and D. F. Bruhn, "On the connectivity anisotropy in fluvial Hot Sedimentary Aquifers and its influence

- on geothermal doublet performance," *Elsevier - Geothermics*, vol. 65, no. January 2017, pp. 222-233, 2017.
- [16] S. Sanaz, R. Al-Khoury, M. N. Hamidreza and M. A. Hicks, "A prototype design model for deep low-enthalpy hydrothermal systems," *Elsevier - Renewable Energy*, vol. 77, no. May 2015, pp. 408-422, 2015.
- [17] C. Willems, H. Hamidreza, T. Goense and D. Bruhn, "The impact of reduction of doublet well spacing on the Net Present Value and the life time of fluvial Hot sedimentary Aquifer Doublets," *Elsevier - Geothermics*, vol. 68, no. July 2017, pp. 54-66, 2017.
- [18] F. Barends, "Complete solution for transient heat transport in porous media, following Lauwerier's concept," *SPE*, vol. SPE Annual Technical Conference and Exhibition held in Florence, no. September 2010, pp. -, 2010.
- [19] N. H. M., S. R., G.-N. M. and J. K., "Modeling transverse dispersion and variable density flow in porous media," *Transport in Porous Media*, vol. 78, no. 1, pp. 11-35, 2009.
- [20] J.-D. van Wees, A. Kronimus, M. van Putten, M. Pluymaekers, H. Mijnlief, P. van Hooff, A. Obdam and L. Kramers, "Geothermal aquifer performance assessment for direct heat production - Methodology and application to Rotliegend aquifers," *Netherlands Journal of Geosciences*, vol. 91, no. 4, pp. 651-665, 2012.
- [21] J. Merva, "Seeking Alpha," Seeking Alpha, 3rd January 2017. [Online]. Available: <https://seekingalpha.com/article/4034075-oil-economics-much-oil-gas-well-cost>. [Accessed 5th June 2019].

- [22] Netherlands Enterprise Agency, "SDE+ Spring 2019," Ministry of Economic Affairs and Climate Policy, Hanzelaan, 2019.
- [23] W. C.J.L. and N. H. Hamidreza, "Towards optimisation of geothermal heat recovery: An example from the West Netherlands Basin," *Elsevier*, vol. 247, no. 2019, pp. 582-593, 2019.
- [24] O. A. Cirpka, "m2matlabdb," MathWorks - Matlab, 3rd April 2003. [Online]. Available: [http://m2matlabdb.ma.tum.de/download.jsp?MC\\_ID=5&MP\\_ID=31](http://m2matlabdb.ma.tum.de/download.jsp?MC_ID=5&MP_ID=31). [Accessed 10th April 2019].
- [25] B. Masoud and M. N. Hamidreza, "Performance of low-enthalpy geothermal systems: Interplay of spatially correlated heterogeneity and well-doublet spacings," *Applied Energy*, Vols. -, no. May 2019, pp. -, 2019.